Development of a high-throughput assay for fatty acid decarboxylases

Jama Hagi-Yusuf

A Thesis

In

Department

Of

Biology

Presented in Partial Fulfillment of the Requirements

for the Degree of Master of Science (Biology) at

Concordia University

Montréal, Quebec

March 2021

CONCORDIA UNIVERSITY
School of Graduate Studies

This is to certify that the thesis prepared

By: Jama Hagi-Yusuf

Entitled: Development of a high-throughput assay for Fatty Acid Decarboxylase

and submitted in partial fulfillment of the requirements for the degree of

Master of Science (Biology)

complies with the regulations of the University and meets the accepted standards with respect to originality and quality.

Signed by the final Examining Committee:

_____ Chair
Dr. Vincent Martin

_____ External
Dr. Steve Shih

_____Examiner
Dr. Peter Pawelek

_____Examiner
Dr. Vincent Martin

_____Supervisor
Dr. David Kwan

Approved by _____

Dr. Robert Weladji

Date _____

Dr. Pascale Sicotte

ABSTRACT

Development of a high-throughput assay for fatty acid decarboxylase

Jama Hagi-Yusuf

Biorenewables have the potential to move society's dependence away from petrol-based industrial products, towards cleaner and more sustainable sources. The technology has moved from focussing on low energy density ethanol- or butanol-based fuel sources to more complex, energy rich hydrocarbons. Recently, a heme-dependent P450 decarboxylase enzyme, $OleT_{JE}$, was discovered in the bacterium *Jeotgalicoccus* sp 8456. This enzyme catalyzes the decarboxylation of a broad-range of long-chain fatty acids producing terminal alkenes that are key energy-rich hydrocarbons valuable for biofuels. Here, we developed an absorbance-based high-throughput assay that facilitated the determination of the activity and Michaelis-Menten kinetics of $OleT_{JE}$. We screened $OleT_{JE}$ decarboxylation by detecting CO_2, a product of decarboxylation. In this assay, CO_2 was converted to bicarbonate and then catalyzed by phosphoenolpyruvate carboxylase and malate dehydrogenase to malate, leading to a decrease in NADH, the detecting molecule. This assay was then used to screen a mutant $OleT_{JE}$ and a non-P450 decarboxylase, to showcase its versatility to screen mutant variants and other decarboxylases.

ACKNOWLEDGEMENTS

I would like to thank my supervisor, Dr. David Kwan, for his guidance, support and understanding through my degree. I have learned how to think and plan like an experimentalist, because of his wisdom and experience. I would also like to thank my committee, Dr. Vincent Martin and Dr. Peter Pawelek, and Dr. Steve Shih my external committee member.

I would like to thank my current and past lab members Laura, Ifthiha, Logan, Trisha, Haoyu, Maxim, Xiaohua, Garbriel and Lan for the support, fun times and help in the lab. I'd like to thank Muhammad from the Kwan and Martin lab for taking plates out for me, being a sound board for my project and grabbing ice cream with me during our incubation times.

I would like to thank Meghan and Lauren from the Martin Lab, and Anic and Dr. Yves Gelinas for the help with the GC/MS, and Ali Fendri from Université de Montréal for help with P450 purification. Thank you to Marie-Eve from Université de Laval for purifying the sinapic acid decarboxylase.

Lastly, I would like to thank my friends and family for their continued support outside of the lab. Thank you to my roommates Sam, Brenda and Jordan for feeding me pizza and helping me relax. Thank you to Jaydon, Turrel, Andre and the rest of the Lloydie's staff for taking my shifts when I was stuck in the lab and your support. Thank you to Hina, Julia, Nnedi, Ceci, Raha and Udbi for your friendship and guidance these last few years. Thank you to Gabriel, Yemisi, Candice and Kadim for your comfort, warmth, spontaneity and joy you always leave me with. Thank you Bofta, Thane, and Timaaj for being a source of strength throughout my Master's.

Finally, thank you to my Hooyo, Ayeeyo and Abo for nurturing my love of science ensuring that I could always imagine being here.

Contributions

I would like to thank all of the people that have helped in the development of this project.

1) The design of the PEPC-MDH assay in Chapters 3.1 and 3.2 were developed by Dr David Kwan and Jama Hagi-Yusuf. In these Chapters, Jama Hagi-Yusuf conducted the experimentation, and analysis of the data.
2) In Chapter 3.3, the enzyme Sinapic Acid Decarboxylase was purified and sent to us by Marie-Ève Picard from the Rong Shi lab at Université Laval.
3) In Chapter 3.3.4, the experimentation was conducted by Dr. David Kwan and Jama Hagi-Yusuf. The dynamic range of Sinapic Acid Decarboxylase in the assay and the rate of reaction at different concentrations of substrate were done by Dr. David Kwan. The data analysis of Chapter 3.3.3 was conducted by Jama Hagi-Yusuf.

Table of Contents

List of Figures

List of Tables

List of Abbreviations

P450 fatty acid decarboxylase from *Jeotgalicoccus* sp ($OleT_{JE}$)

Phosphoenol pyruvate (PEP)

Phosphoenol pyruvate carboxylase (PEPC)

Malate dehydrogenase (MDH)

Nicotinamide adenine dinucleotide (NADH/NAD+)

Dithiothreitol (DTT)

Phenolic acid decarboxylase (PAD)

Sinapic acid decarboxylase (SAD)

Chapter 1: Introduction

Worldwide concern over global warming has been rising with the increasing temperatures resulting from human activity and industry involving the burning of fossil fuels (Bush & Flato, 2019). The rise in global mean temperature has devastating effects on society and human life. The environmental effects are seen around the planet, yet can affect distinct populations differently and often disproportionately (Nazrul Islam & Winkel, 2018). Somalia, my parent's country of birth, has been impacted by multiple, long droughts over the course of the last 10 years. Beginning in 2010, a record drought that led to a famine in the region of mostly nomads resulted in more than a quarter million deaths and 2.1 million displaced refugees. Droughts are not foreign to the region, but their frequency and intensity has increased over the last decade and climate scientists have concluded that this is due to the effects of global warming (Jayawardhan, 2017). Somalia is not the only nation to be impacted by climate change, the Earth's global mean temperature has risen in the last century by 0.8 °C, 1.7 °C in Canada and 2.3 °C in Northern Canada (Bush & Flato, 2019). In Northern Canada, the food security, physical health and mental health of Indigenous communities have been greatly affected by a changing climate (Ford, 2009; Middleton *et al*., 2020; Watts *et al*., 2017).

Global warming has been strongly linked to anthropogenic activity with high confidence levels, mainly due to rising levels of greenhouse gases (Bush & Flato, 2019). The global net increase in greenhouse gases has motivated scientists and community leaders to rethink humanity's relationship to the planet and to its resources.

Much of the global economy, infrastructure, and technologies are currently dependent on fossil fuels. In 2018, CO_2, a by-product of the combustion of fossil fuels, accounted for 80% of Canada's greenhouse gas emissions (Environment and Climate Change Canada, 2020). Beyond fuels, petroleum mixtures provide precursors to many valued materials and fine chemicals, such as plastics, surfactants, clothing, cosmetics, and soap (Fillet & Adrio, 2016; Ladygina, Dedyukhina, & Vainshtein, 2006; Nomura & Taguchi, 2007). Synthetic biology can provide us with the means to produce these resources sustainably.

1.1 Synthetic Biology and Renewable Resources

Synthetic biology is a discipline in biology that has pushed a paradigm shift in biotechnology and genetic engineering, where chemistry, mathematics, computer science, and other fields have advanced the frontiers of the discipline. It has been described by Christopher Voigt as an engineering discipline with "a desire to build things that do not yet exist" (Church, Elowitz, Smolke, Voigt, & Weiss, 2014). Early synthetic biologists began with the development of switches to control cellular activity, that were developed using mathematical simulations and standardization of genetic components of the switch (Gardner, Cantor, & Collins, 2000). It has now expanded to complex networks with wide applications in medicine, energy, renewable resources and agriculture.

Many bacteria, fungi, and other microorganisms produce fine chemicals and precursors to valued materials from bio-based resources, which can potentially replace petroleum dependency (Liao, Mi, Pontrelli, & Luo, 2016). The strategies to take advantage of this have included bio-prospecting, host optimization, fermentation, and metabolic and protein engineering (Atsumi,

Cann, *et al*., 2008; Garrison, Murawski, & Quirino, 2016; Jiang, Gu, & Zhang, 2018a; Liu & Li, 2020; Wang *et al*., 2018). There has been a strong effort to increase the yields of these products to be cost-efficient and sustainable with synthetic biology approaches.

1.2 Bio-polymers

Petroleum-based polymers and specialty fine chemicals make up less than 5% of the total volume of extracted petroleum; however, they make up 42% of the market value (Hernández, Williams, & Cochran, 2014). These polymers are applied to make casings, containers, packaging, textiles and many other uses (Garrison *et al*., 2016). Annually, this accounts for 300 million tons of the world's oil and natural gas supply (Hernández *et al*., 2014). There has been new interest to develop valued polymers from biological sources in recent years.

From paper to clothing, humans have used biological sources to produce materials of value. Plant- and animal-based products have wide and diverse applications from food and health to material industries (Garrison *et al*., 2016; Xia & Larock, 2010). Some of the monomers that are derived from petroleum, which are then catalyzed to polymeric materials, can be found endogenously in microbes, plants, and fungi at low quantities (Adkins, Pugh, McKenna, & Nielsen, 2012). With Synthetic Biology, these microbes can be engineered to increase their production of the sought-out monomers which can then be chemically polymerized to make complex materials such as polylactic acid, polyester, and polyamide (Adkins *et al*., 2012). In this new paradigm shift, moving away from the harms of petroleum, synthetic biology-based approaches may provide alternatives to petroleum-based products.

Styrene is one of many high-valued monomers derived from petrochemicals that polymerize to polystyrene and other polymers. Ethylbenzene, a compound derived from petroleum, is dehydrogenated via steam to produce styrene which is an energy-intensive process (Adkins *et al*., 2012). It is also found endogenously in many plant and fungi species, which can provide a more renewable avenue of styrene production. McKenna *et al*. co-expressed enzymes from *Arabidopsis thaliana* and *Saccharomyces cerevisiae* in *Escherichia coli* and successfully produced styrene titers (McKenna & Nielsen, 2011). Similar methods of metabolic engineering, where heterologous pathways have been introduced into a microbial chassis, have been used to increase production of different monomers that can then by polymerized to industrial materials. This provides us with an advantage over petroleum-derived polymers, where new biopolymers with unique properties can be built from the bottom-up.

Polylactic acid (PLA) and polyhydroxyalkanoates (PHA) are two microbially-derived polyesters of interest in medicine due to their biodegradability and versatility (Doppalapudi, Jain, Khan, & Domb, 2014; Iwata, 2015; Jain, Sokolsky, Kumar, & Domb, 2008). With these properties in mind, they have been used in surgical devices, sutures, drug delivery, implants, tissue engineering, and many other invasive medical devices (Doppalapudi *et al*., 2014; Iwata, 2015; Jain *et al*., 2008; Langer, 1990). PHAs are the carbon and energy storage polymers of many bacteria resulting from the polymerization of hydroxyalkanoic acids, while PLAs are polymerized and processed from lactic acid monomers produced by bacteria (Hamad, Kaseem, Ayyoob, Joo, & Deri, 2018; Nomura & Taguchi, 2007).

Lactic acid is produced in the acid- and thermo-tolerant lactic acid bacteria (LAB) families and it has also been found in non-LAB bacteria such as *E. coli* and *Bacillus* sp (Axelsson *et al*., 2012). Heterologous expression of the xylose assimilating *xylAB* operon from *Lactobacillus pentosus* into *Lactobacillus plantarum* led to a titer of 120g/L of lactic acid from delignified hardwood pulp due to improved sugar utilization in the pathway (Axelsson *et al*., 2012). Genetic modifications allowed for improved titers but also selectivity in yielding a product. Expression of either D- or L- lactate dehydrogenase in *Pediococcus acidilactici* DQ2 leads to selective production of D- or L- lactic acid solving the problem of unstable polymers from racemic lactic acid mixtures and to more controlled polymerization (Axelsson *et al*., 2012). Unlike PLAs, PHAs are polymerized in the cells and reduces the chemical processing step in producing the plastic. However, that also comes with more difficulty in controlling the polymer produced in the cell. To reduce structural variation to PHA, the β-oxidation pathway in *Pseudomonas entophila* L43 was deleted and this show-cased consistent polymer production dependent on fed-substrate (Li *et al*., 2014; R. Shen *et al*., 2014). Many methods have been employed to control and increase production of PHAs and PLAs via engineering the pathways and the enzymes that lead to them.

Companies like Cargill, DuPont and others have aimed to sustainably develop fine chemicals. DuPont Sorona successfully created a cost-competitive biopolymer through microbial engineering that has been used in apparel, carpeting and packaging applications (Betts, 2015). The advancement of biopolymers to replace petrochemical-derived polymers is dependent on improving the cost-efficiency and mass production of biopolymers due to the low-cost of these petroleum polymers. The goal to transition global industries away from petroleum-based

products is not limited to materials alone. Similar strategies to biopolymer production in microbes have been employed to efficiently produce biofuels to replace global dependency on fossil fuels.

1.3 Biofuels

Automotive fuels like gasoline can be judged by a few criteria, such as the octane number, the resistance of spontaneous ignition between fuel and air mixtures (knocking), and energy content of the fuel, which is largely dictated by the carbon chain length and carbon-hydrogen bonds (Lee, Chou, Ham, Lee, & Keasling, 2008). In early developments of biofuels, ethanol was proposed as a potential fuel source. While ethanol has a higher octane number than gasoline, it is only 70% of the energy content of it (Lee *et al*., 2008). Another concern with ethanol is its high miscibility with water making the extraction, storage and transportation difficult (Lee *et al*., 2008).

In the development of a biofuel source, the criteria above are used to note the feasibility of the potential fuel source. As a fuel source that can replace gasoline, ethanol would not be practical. However, the addition of ethanol to gasoline mixtures was shown to reduce overall emission levels since it can improve fuel combustion as an oxygenase (Sawyer, 1993).

Longer-chained carbon molecules such as short-chain alcohols or hydrocarbons with higher energy densities that are comparable to gasoline, are a focus today in the advancement of new biofuels (Savage, 2011). ‘Drop-in’ biofuels are biofuels that can replace modern gasoline mixes without any drastic mechanical change to the automobile (Savage, 2011). The compounds of

interest that can potentially make-up the 'drop-in' biofuels have been identified in nature and they require further bioengineering to attain cost-effective titers **(Table 1)**.

1.3.1 Short-Chain Alcohols

Gasoline is a mixture of carbon molecules of lengths C4-C12 and short-chain alcohols (C4-C8) have been proposed as potential replacements to fuel systems since they have energy contents and octane numbers that are comparable to gasoline (Lee *et al*., 2008). *n*-Butanol, a 4-carbon chained alcohol, is endogenously produced in *Clostridium sp* along with other similar short-chain alcohols like isobutanol and *n*-propanol, which are promising biofuel candidates due to their carbon lengths (Lamsen & Atsumi, 2012). These short-chained alcohols have been produced in microbes through the alpha-keto acid pathway or the non-decarboxylative Claisen condensation pathway (Jiang *et al*., 2018).

The alpha-keto acid pathway is primarily involved in amino acid biosynthesis and the alcohols are derived from catalyzing reactions of the alpha-keto acid intermediates in the pathway. The intermediates are catalyzed via amino acid decarboxylase and reduced with alcohol dehydrogenase. Atsumi and Liao, engineered *E. coli* to select for higher levels of 2-ketobutyrate, a precursor to 1-propanol and 1-butanol (Atsumi, Hanai, & Liao, 2008). This approach, coupled with overexpression of heterologous α-ketoisovalerate decarboxylase (KivD) and alcohol dehydrogenase (ADH2) enzymes, increased titers of 1-propanol and 1-butanol by a factor of 9 and 21, respectively (Atsumi, Hanai, *et al*., 2008).

Engineering of the alpha-keto acid pathway has led to higher levels of short-chain alcohols, with 22g/L of isobutanol from Atsumi's previous work (Atsumi, Cann, *et al*., 2008). Metabolic engineering techniques to optimize expression of the short-chain alcohols generally follow a similar strategy of (i) heterologous expression of amino acid decarboxylase or alcohol dehydrogenase, (ii) deletion or overexpression of enzymes in the pathway (iii) carbon flux directed to increase intermediates of alpha-keto acid pathway, (iv) protein engineering of enzymes in the pathways.

The non-decarboxylative Claisen condensation pathway discovered in *Clostridium kluyveri*, similarly can produce short-chain alcohols via a step-by-step process to increase carbon length through the terminal acyl group (Barker & Taha, 1941; Jiang *et al*., 2018).The pathway uses two acetyl-CoA substrates and condenses them with a thiolase to acetoacetyl-CoA, which can be further catalyzed by β-reduction reactions (Jiang *et al*., 2018). It was reverse-engineered by Dellomonoca *et al*, to build fatty acids, alcohols and other complex hydrocarbons via reversing the β-oxidation pathway (Dellomonaco, Clomburg, Miller, & Gonzalez, 2011; Jiang *et al*., 2018).

In *E. coli*, the engineered pathway was able to produce up to 30 g/L of 1-butanol, 30x higher than the highest titer from the alpha-keto acid pathway (Jiang *et al*., 2018; Shen & Liao, 2008; Shen *et al*., 2011). This versatile system can allow for longer acyl-chains to form through simple step reactions and provides a platform to add functional groups to the growing chains. It creates multi-chained hydrocarbons, thus creating more complex fine chemicals, such as 2-

methylpentanoic acid and 2,3-dihydroxybutyric acid (Cheong, Clomburg, & Gonzalez, 2016; Jiang *et al*., 2018).

The additive, simple and flexible system that the condensation pathway uses, produces longer-chained hydrocarbons that provide more diverse properties to fine chemicals. Using this system, fatty acids, C6-10 were produced with titers of 3.8g/L (Wu, Zhang, Xia, & Dong, 2017). Gasoline, jet fuel and biodiesel are a mixture of varying hydrocarbon lengths. The alpha-keto acid pathway and non-decarboxylative condensation pathway are limited in that they cannot produce the higher-end chains in these mixtures. Different microbial metabolic pathways have been identified that produce longer-chained hydrocarbons found in petroleum (**Table 1**).

Table 1: Enzymes that produce short-chain alcohols and oleochemicals of interest in the biofuel industry

Enzyme(s)	*Product of Interest*
2-ketoacid decarboxylase and aldehyde/alcohol dehydrogenase **(***Clostridium acetobutylicum***)**	1-propanol (C_3) (Atsumi, Hanai, *et al*., 2008) 1-butanol (C_4) (Atsumi, Hanai, *et al*., 2008) Isobutanol (C_4) (Atsumi, Hanai, *et al*., 2008) 2-methyl-1-butanol (C_5) (Atsumi, Hanai, *et al*., 2008) 2-phenylethanol (C_8) (Atsumi, Hanai, *et al*., 2008)
Medium-chain specific fatty acid thioesterase (*E. coli*)	Medium-chain length fatty acid (C_6-C_{10}) (Hu, Zhu, Nielsen, & Siewers, 2019)
Engineered Fatty Acid Synthase I (*Saccharomyces cerevisiae*)	Medium-chain length fatty acid (C_4-C_9) (Hu *et al*., 2019)
P450 OleT (*Jeotgalicoccus sp.*)	Terminal alkenes (C_3-C_{19}) (Rude *et al*., 2011)
UndA (*Pseudomonas spp.*)	Terminal alkenes (C_9-C_{13}) (Rui *et al*., 2014)
UndB (*Pseudomonas spp*.)	Terminal alkenes (C_5-C_{18}) (R. Shen *et al*., 2014)
Ols/Type-1 PKS (*Synechococcus sp. strain PCC 7002*)	Terminal alkenes ($C_{19:1}$,$C_{19:2}$) (Mendez-perez, Herman, & Pfleger, 2014)
Aldehyde deformylating oxygenase (*Synechoccus elongatus* PCC7942)	Alkane (C_3-C_{17}) (Schrimer, Rude, Li, Popova, & Del Cardayre, 2010)
P450 Aldehyde Decarbonylase (*Drosophila melanogaster*)	Alkane (C_{23}-C_{28}) (Qiu *et al*., 2012) Alkane (C_1-C_{17}) (Sorigué *et al*., 2017)
Fatty Acid Photodecarboxylase (*Chlorella variabilis*)	

1.3.2 Biologically-derived Oleochemicals and Hydrocarbons

Oleochemicals consist of molecules with medium- or long-chain alkyl groups that are primarily derived from vegetable or animal lipids and fats and are considered to be an alternative to petroleum, such as biodiesel (being compatible with conventional diesel engines). Oleochemicals share many of the desirable properties of hydrocarbons, such as fuels with their high energy density. Hydrocarbons, which consist only of carbon and hydrogen atoms, are typically derived from petroleum. However, many hydrocarbons are naturally occurring in living organisms. They consist of aliphatic alkanes and alkenes, aromatic hydrocarbons and many other molecules that are found within plant and microbial species (Hu *et al*., 2019). These chemicals are of interest in cosmetics, thickeners, and plasticizers. Importantly, medium-chain (C8-C12) length biologically-derived oleochemicals and hydrocarbons can theoretically replace fossil fuels such as gasoline, jet fuel and diesel (Jiang *et al*., 2018).

Multiple engineering techniques have been identified to successfully produce medium-chain length fatty acid derivatives. In *E. coli*, medium-chain specific fatty acid thioesterases produced medium-chain length fatty acid, while in *Saccharomyces cerevisiae* fatty acid synthase I (FASI) had been rationally engineered to restrict its chain lengths and produce medium-chain length fatty acids (Jiang *et al*., 2018). Heterologous expression in *E.coli* and *S. cerevisiae* have significantly improved titers of fatty acids and other fatty acid derivatives and further rewiring of the fatty acid biosynthesis pathway has improved titers as well (Hu *et al*., 2019). However, fatty acid derivatives do not constitute the majority of fossil fuel mixtures today.

Medium-chained alkanes and alkenes are the major constituents of gasoline and similarly to other biohydrocarbons they are found in low-levels in microbes (Hu *et al*., 2019). Microbially-derived alkanes and alkenes are generated from fatty acid derivatives and improving their titers consists of increasing the carbon flux to their precursors (fatty acids, fatty aldehydes, and fatty acyl-CoA/ACPs) and increasing catalysis by an enzyme to either alkanes, terminal alkenes or internal alkenes (Liu *et al*., 2016; Wang *et al*., 2018).

The alkane biosynthetic pathway was first discovered in *Cyanobacteria*, where the operons identified in alkane production were expressed in *E. coli* and *Asperigillus carbonarius* producing alkane titers of 0.3 g/L (C13-17) and up to 10.2mg/mL (C15-C17), respectively (Hu *et al*., 2019; Wang *et al*., 2018). Tampering with the fatty acid biosynthetic pathway can negatively impact the growth of *S. cerevisiae*, localizing the alkane biosynthetic pathway into the peroxisomes was a successful strategy to isolate the heterologous pathway from the endogenous and competitive pathway in the cytosol (Hu *et al*., 2019; Zhou *et al*., 2016).

Other pathways have been recently discovered in insects and plants, and heterologous expression of these enzymes have also led to higher titers of alkanes and alkenes in microbial hosts. Alkane and alkene production needs to be further characterized in microbial hosts with these new enzymes. Alkenes are economically valuable because they increase the combustion process of gasoline and it's octane number (Hajbabaei *et al*., 2013). In 2011, Rude *et al*. discovered a P450 peroxygenase, $OleT_{JE}$, in the bacterium *Jeotgalicoccus sp* ATCC 8456 and learned that it is capable of catalyzing the decarboxylation of free fatty acids, producing terminal alkenes, making $OleT_{JE}$ an enzyme of interest in the development of drop-in biofuels (Rude *et al*., 2011).

1.4 P450 Terminal Olefin Producing Enzyme, OleT

To further understand alkene biosynthesis, Rude *et al*. used a reverse genetic approach in the genus *Jeotgalicoccus* to identify a P450 fatty acid decarboxylase ($OleT_{JE}$) (Rude *et al*., 2011). The enzyme produces terminal alkenes efficiently from linear fatty acids between 10 to 20 carbons in length. $OleT_{JE}$ mainly decarboxylates fatty acids, unlike other members of the CYP152 family favour hydroxylation (Rude *et al*., 2011; Belcher *et al*., 2014). Drop-in biofuels have been the main interest for the alkene products of $OleT_{JE}$, but the enzyme's ability to convert fatty acids into terminal alkenes can be useful for producing molecules that may have industrial value in other applications, for example as surfactants or lubricants.

Most P450s catalyse redox reactions and they typically use NADH or NADPH as electron donors, in conjunction with a bound di-oxygen to a heme (Bogaert, Groeneboer, Saerens, & Soetaert, 2011). Some P450s, like $OleT_{JE}$ and other P450 peroxygenases in the CYP152 family, are able to use H_2O_2 as an electron donor instead that efficiently catalyze these reactions without damaging their heme (Rude *et al*., 2011). The catalytic mechanism of P450 heme is generally consistent among the family; however, peroxygenases take advantage of the peroxide shunt to donate two electrons (**Figure 1; Figure 2**).

By using the peroxide shunt, the reaction bypasses one of the uncoupling mechanisms the "auto-oxidation" shunt where the ferric superoxide is auto-oxidized and returns to the high spin state which inactivates the heme. H_2O_2 can be used as an electron donor for most P450s; however, it is inefficient and leads to enzyme inactivation (Hammerer, Winkler, & Kroutil, 2018).

Peroxygenases from the CYP152 family have evolved to use the peroxide shunt to achieve the necessary heme states for catalysis (Hammerer *et al*., 2018).

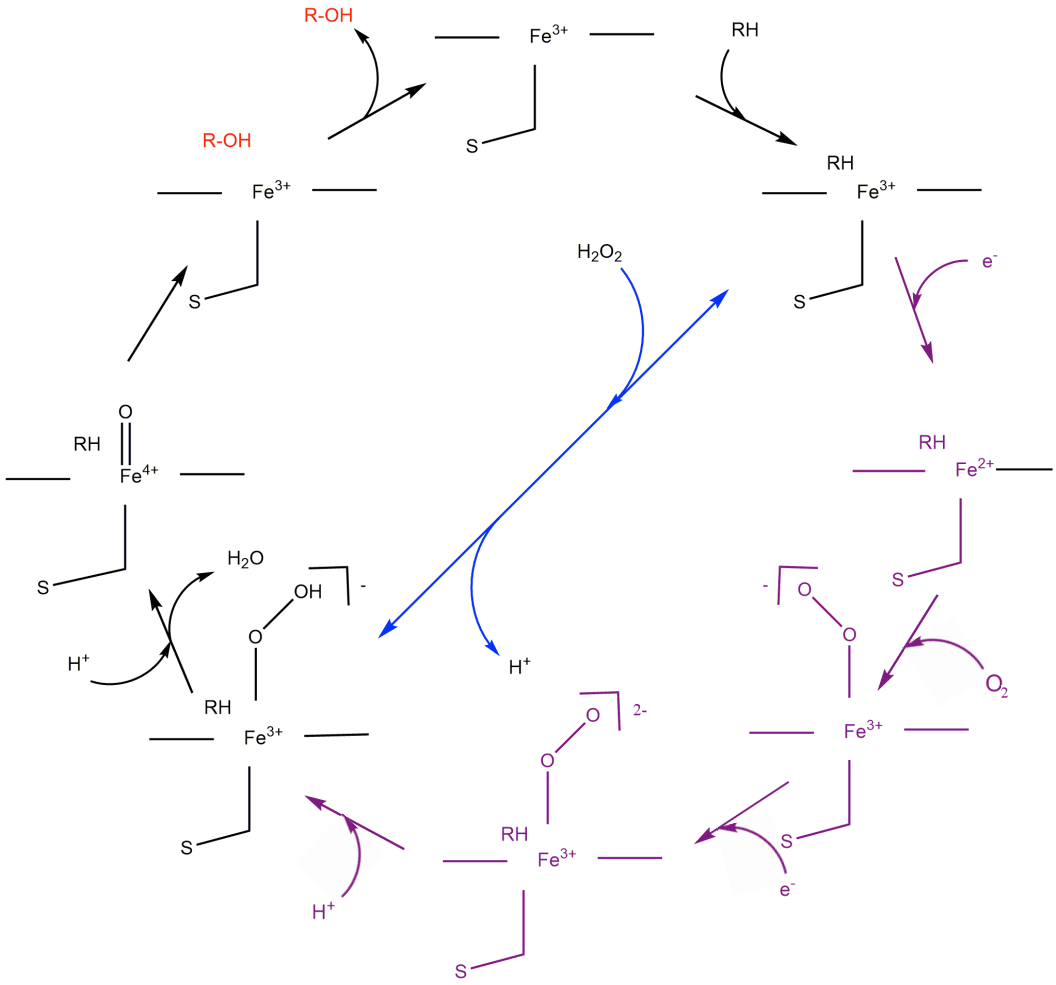

Figure 1. The catalytic mechanism of P450 OleT$_{JE}$ heme.

The substrate displaces water from the heme which cascades the reaction. The heme moves from the high-spin state Fe^{3+} state to the ferric-hydroperoxo complex, Compound 0 through the peroxide shunt pathway. The catalytic route of non-peroxygenase P450s uses a series of reduction, oxygenation and protonation steps to reach compound 0 (purple).

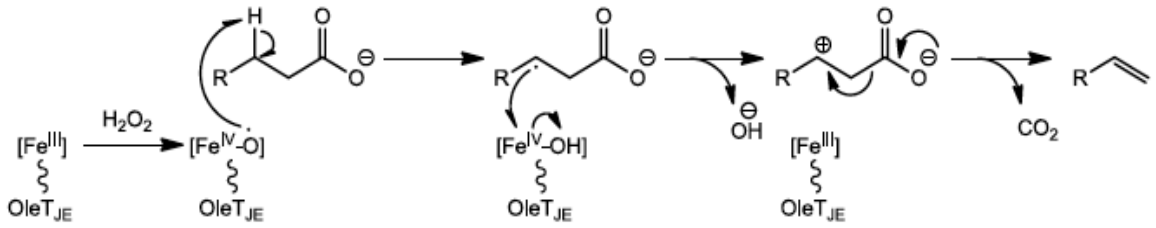

Figure 2. A prediction on the decarboxylation mechanism of $OleT_{JE}$.
The reactive state of the P450 heme, Compound 1, will abstract a H from from the β-carbon which triggers a decarboxylation event.

Structural analysis between peroxygenases and other P450s provides some potential insight into the differences between the catalytic mechanisms. The P450 pocket contains acid-alcohol amino acid pair, asparagine and threonine, involved in proton transfer with the iron-oxo catalytic cycle (Munro, McLean, Grant, & Makris, 2018). In the CYP152 family, the conserved amino acids appear to be arginine and proline in the family as well as the loss of a conserved phenylalanine residue in the heme-binding loop (Munro *et al*., 2018). This suggests a far divergence from the wider P450 family along with the H_2O_2-driven catalysis (Munro *et al*., 2018).

Although, $OleT_{JE}$ has close similarities to other P450 peroxygenases, there are some points of difference that most likely lead to the enzyme favouring decarboxylation over hydroxylation. The active site has the conserved Arg245 bound to the carboxylate group of the fatty acid substrate (Belcher *et al*., 2014). The entrance of the binding pocket of $OleT_{JE}$ has a 3-residue difference, Thr-24, Ala-40 and Ala-317, from other fatty acid peroxygenases, Ile-25, Leu-41 and Leu 315, that expand the pocket to allow larger fatty acid substrates (Belcher *et al*., 2014).

Many groups have attempted to utilize $OleT_{JE}$ to make terminal alkenes for their economically relevant biorenewables and biofuels. Yan *et al* improved the yield of terminal alkenes from renewable triacylglycerols in a simple two-step pathway, where they cloned lipase from *Thermomyces lanuginoses* and $OleT_{JE}$ in *S. cerevisiae* (Yan, Liu, Wang, Han, & Li, 2015). In continuation of this work, the group fused the lipase and $OleT_{JE}$ to an *in vitro* multi-enzyme complex that binds to a cellulose carrier (Li *et al*., 2019). The complex produced more alkenes than the unbound forms of the enzymes, and increased stability in different pH, higher temperatures and different organic solvents (Li *et al*., 2019). To improve the catalytic activity of $OleT_{JE}$, Liu *et al* linked the C-terminal of $OleT_{JE}$ with a NADPH-dependent reductase from *Rhodococcus* sp. NCIMB 9784, to create a H_2O_2-independent $OleT_{JE}$ (Liu *et al*., 2014). While the fusion worked well and had displayed slight differences in substrate specificity, ultimately wild type $OleT_{JE}$ created the highest titers (Liu *et al*., 2014). However, they displayed a potentially new system to study $OleT_{JE}$. Different strategies to study or improve activity of $OleT_{JE}$ have been employed, however very few have attempted to mutate the enzyme.

There have been few attempts to increase 1-alkene titers for $OleT_{JE}$ through mutagenic methods, since many of the analytic methods of $OleT_{JE}$ are low-throughput analytic tools. There are many methods that can be employed in the engineering of $OleT_{JE}$. Directed evolution methodologies take advantage of evolutionary principles and the methodology depends on the information available of the protein and the desired function.

1.5 High-Throughput Screening Methods

High-throughput screening and selection methods are important in the identification of novel and desirable protein function and are needed in discovering these functions through a mutant library (Xiao, Bao, & Zhao, 2015). Low-throughput selection or screening methods would take too long to isolate novel protein function in a large library, which can take millions of mutant variants-depending on the engineering system employed (**Figure 3)**. Essentially, screening methods are ways of identifying sought-out functions through evaluating every protein and selection methods are ways of eliminating undesirable phenotypes (Xiao *et al*., 2015). Screening and selection methods have to be developed dependent on the desired protein engineered. HTS methods can employ plate-based or cell-based methodologies to detect new activities.

Cell-based assays require a detectable signal within cells to select or screen for desired functionality, such as fluorescence, absorbance, or growth under selective conditions. High-throughput assay strategies, like fluorescence-activated cell sorting (FACS), have the capability of sorting through large libraries of cells and detecting fluorescent signals. For example, towards biorenewable energy, Barhona *et al*. engineered a Molybdenum-dependent nitrogenase through random mutagenesis to create a H_2- over-producing strain of *Rhodobacter capsulatus* (Barahona, Jiménez-Vicente, & Rubio, 2016). Upon production of H_2, *lacZ* is transcribed where LacZ catalyzes the hydrolysis of fluorescein di-β-galactose to release fluorescein, allowing cells to be detected by FACS (Barahona *et al*., 2016).

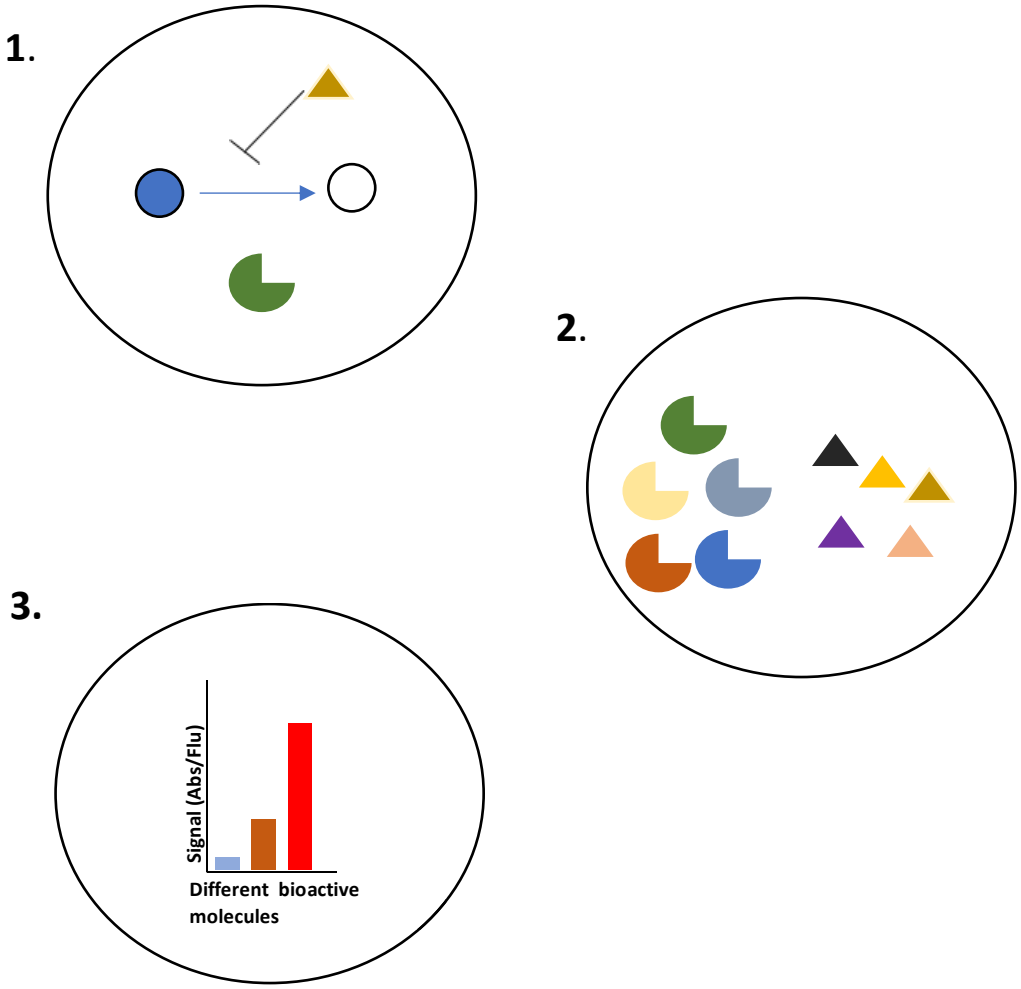

Figure 3. A simple break-down of high-throughput screening methods.
1) Bioactivity must be linked to a detectable signal (Absorbance, Fluorescence, Growth) to be able to measure a change in bioactivity. 2) A large library of bioactive molecules where the high-throughput method can detect differences in bioactivities between the molecules (enzymes, inhibitors, substrates) 3) Analysis of the results from the high-throughput method in the large library.

In another example of enzyme directed evolution using FACS, Aharoni *et al* developed a high-throughput screen to detect improved sialyltransferase activity *in vivo* from *Campylobacter* by engineering JM107 to transport Neu5Ac donor and lactose acceptor efficiently (Aharoni *et al*., 2006). This system allowed the sialyltransferase to sialylate the fluorescent acceptors, trapping the sialylated-fluorescent molecule in the cell where FACS successfully detected the difference against a control (Aharoni *et al*., 2006).

While cell-based assays are advantageous since studying enzymes *in vivo* are more likely to give accurate results in practice, these strategies need to be devised in such a way that allows for activity to be observed in living cells, which may be challenging. Some systems are more efficiently detected in plate-based, *in vitro*, assays to characterize activity. Plate-based assays, like cell-based assays, detect signal changes as a means of quantifying differences in bioactivity. The assays range of sensitivity, interference by other reactants or products, buffer considerations and other reaction components are important to be identified and optimized.

In an example using plate-based high-throughput screening applied to engineer microbial short-chain alcohol production, Agu *et al*. developed an assay that quantifies butanol in *Clostridium* through conversion of butanol to butryaldehyde by *Thermotoga hypogea* alcohol dehydrogenase (*Th* ADH), where NADPH (a co-factor of *Th* ADH) was detected at 340 nm through spectrophotometry (Agu *et al*., 2018). While the plate-based screen applied is continuous, since NADPH production over time was detected by the spectrophotometer, a fixed-time point was used to compare against the different *Clostridium* strains (Agu *et al*., 2018).

Agu *et al*., Aharoni *et al*., and Barahona *et al*., all employed detectable signals, absorbance or fluorescence, that were linked to enzymatic activity to screen for a specific bioactivity (Agu *et al*., 2018; Aharoni *et al*., 2006; Barahona *et al*., 2016). The development of high-throughput screening systems requires signals to be specific to the bioactivity of interest; however, sometimes researchers require to use some creativity to link bioactivity to a detectable signal.

1.5.1 High-Throughput Assays for Decarboxylases

Decarboxylases are a group of diverse enzymes, phylogenetically and mechanistically. They catalyse the defunctionalization of organic compounds, by cleaving the carboxylic acid groups and releasing a CO_2 (**Figure 4)** (Kourist, Guterl, Miyamoto, & Sieber, 2014). High-throughput assays developed for decarboxylases have been specific to the catalytic mechanism of decarboxylation or the decarboxylated products, which leads to multiple screening platforms developed for these class of enzymes.

A high-throughput colorimetric pH-based assay was developed to detect the activity of glutamate decarboxylase (Yu, Hu, Huang, & Mei, 2011). Bromocresol green was used as an indicator to detect decarboxylase activity, to signal slight pH shifts during catalysis (Yu *et al*., 2011). The buffer and indicator concentrations were optimized to maximize signal sensitivity and buffer stability (Yu *et al*., 2011). The screen rapidly detected glutamate decarboxylase activity, kinetics and showcased its high-throughput potential to screen mutant libraries for 2-fold enzyme activity (Yu *et al*., 2011). While many assays are developed to improve the bioactivity of a phenotype, they are also used to detect inhibitors. Histamine, a product of histidine decarboxylase, is a mediator for allergic, inflammatory and neurological responses in humans (Gautschi *et al*.,

2006). A high-throughput assay was developed via fluorescence polarization to identify and develop drugs that will inhibit histidine decarboxylase activity to target histamine-associated health issues (Gautschi *et al*., 2006). The IC_{50} values of 3 known inhibitors were similar to those previously reported and those identified through HPLC-based screening methods, indicating a successful assay (Gautschi *et al*., 2006).

In 2011, a generalized assay for amino acid decarboxylases was developed to circumvent the time around assay development for each amino acid decarboxylase (Mødici, María, Otten, & Straathof, 2011). The assay was a fluorescence-based screen that utilized the fluorometric response between primary amines, o-diacetylbenzene and mercaptoethanol to detect the decarboxylation of an amino acid (Mødici *et al*., 2011). It successfully detected the activity of a broad-range of amino acids, excluding those with another amine group in the side chain (Mødici *et al*., 2011). The development of high-throughput assays are often the limiting factor in many enzyme applications. Generalized assays would reduce the time taken in assay development which would allow researchers to answer more complex and fundamental questions on an enzyme's activity.

A generalized, non-radioactive high-throughput assay was developed to detect CO_2 in the decarboxylation reaction in an anaerobic chamber (Smithson, Shelat, Baldwin, Phillips, & Guy, 2010). They used the existing PEPC-MDH coupling assay to screen a library of ~ 3600 potential inhibitors of ornithine decarboxylase (Smithson *et al*., 2010). This coupled enzyme assay is used in the detection of dissolved bicarbonate, involving the enzymes phosphoenolpyruvate carboxylase (PEPC) and malate dehydrogenase (MDH). The PEPC-MDH assay is a well-

established coupling assay that has been used to detect CO_2 and HCO_3^- in plant tissues and blood samlples (Smithson *et al*., 2010). The assay has been applied to S-adenosylmethionine decarboxylase, without the use of an anaerobic chamber (C. Liao, Wang, Tan, Sun, & Liu, 2015). The PEPC-MDH assay was showcased as a way to identify potential inhibitors of s-adenosylmethionine decarboxylase to aid in reducing polyamine levels in canercerous cells (Liao *et al*., 2015). This adaptation of the generalized PEPC-MDH assay indicates how the assay can potentially be used in the detection of decarboxylation activity.

1.6 Thesis Objectives

The fine chemicals produced by $OleT_{JE}$ can be a biorenewable source for multiple different industries. The low-level production of the 1-alkenes is not cost-effective for industrial purposes. The alkenes are generally detected using Gas-chromatography/Mass Spectrometry (GC/MS), a low-throughput method, which limits the potential to effectively study $OleT_{JE}$ decarboxylation activity. To tackle this problem, we worked on three aims over the course of my Master's:

1) ***Develop a generalized-assay for decarboxylase activity for $OleT_{JE}$***

Here, the developed high-throughput PEPC-MDH assay was adapted to function outside an anaerobic chamber to detect the decarboxylation reaction. The aim was to create a method to use the screen and continuous assay for decarboxylases without greatly impacting the signal-background ratio.

2) *Apply the PEPC-MDH assay to $OleT_{JE}$*

Once it was shown that the PEPC-MDH assay could detect different $KHCO_3$ levels, demonstrating the possibility that it could be used in a decarboxylase assay, we added $OleT_{JE}$ and carbonic anhydrase (CAase) to the assay. Here, the assay conditions was optimized for $OleT_{JE}$ and determined the Michaelis-Menten kinetics of $OleT_{JE}$. The ultimate goal is to use this assay to screen for large mutant libraries, so we applied the assay to a mutant of $OleT_{JE}$ and compare the behaviour to wildtype.

3) *Apply the PEPC-MDH assay to a non-P450 decarboxylase, Sinaptic Acid Decarboxylase (SAD)*

The PEPC-MDH based assay is a generalized assay and has been previously used to detect decarboxylase activity at higher pHs. Many decarboxylases are buffered below pH 7 and there are few screens available. We apply the assay to show the versatility as a screen and to detect Michaelis-Menten kinetics of sinaptic acid decarboxylase (SAD), a phenolic acid decarboxylase.

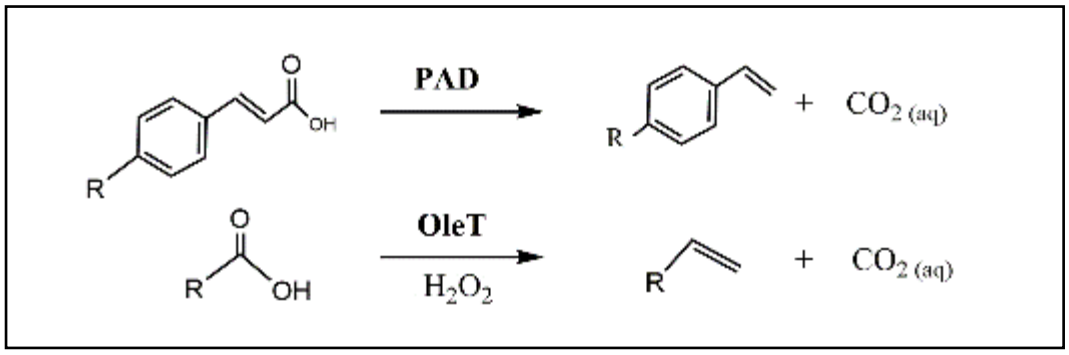

Figure 4. Decarboxylation reaction of $OleT_{JE}$ and Phenolic Acid Decarboxylase.

Chapter 2: Materials and Methods

2.1 Reagents, Media, and Buffer Recipes

See Appendix B for common media and buffer recipes unless otherwise stated, media and buffer components were obtained from Sigma Aldrich or Carbosynth.

2.2 Experimental Methods

2.2.1 PEPC-MDH Assay

The PEPC-MDH assay was adapted to be assayed in atmospheric conditions. To minimize interference, the reaction was divided into three mixes: the enzyme mix, the buffer mix and the final addition of substrate, $KHCO_3$. The mixes were set-up to give final assay conditions of 0.1 mg/mL PEPC, 0.1 mg/mL MDH, 50 mM Tris (pH 8), 0.5 mM $MgCl_2$, 5 mM PEP, 1 mM NADH and at 25°C. The enzyme mix (PEPC and MDH) and buffer (Tris, $MgCl_2$, PEP and NADH) mix were added to the reaction first. The reaction was monitored for 30mins at 25 °C in a ClarioStar spectrophotometer in a 96-well plate where NADH absorbance levels were observed. Once a stable background reading of the change of NADH absorbance was observed (*i.e.*, once the majority of dissolved CO_2 was consumed), $KHCO_3$ was added to the reaction wells.

2.2.2 $OleT_{JE}$ Assay

The $OleT_{JE}$ assay followed a similar protocol as the "PEPC-MDH" assay, where the reaction mix was divided into 4 different volume additions. The mixes were set-up to give final assay conditions of 0.1 mg/mL PEPC, 0.1 mg/mL MDH, 0.1 mg/ML carbonic anhydrase, 50 mM Tris-HCl (pH 7), 0.5 mM $MgCl_2$, 5 mM PEP, 1 mM NADH, 0.5 mM H_2O_2, 10% DMSO and at 32°C. The 1x enzymes mix, PEPC, MDH, carbonic anhydrase, the 2x buffer mix containing the co-

substrates (PEP, $MgCl_2$, NADH, DMSO, and myristic acid), and 1x $OleT_{JE}$ were added. Once the stable background reading of the change in NADH absorbance was observed, H_2O_2 was added to the reaction wells to initiate the $OleT_{JE}$ reaction.

2.2.3 PAD Assay

The PAD assay followed a similar protocol to the "PEPC-MDH" assay, where the reaction mix was divided into 3 mixes. The mixes were set-up to give final assay conditions of 0.1 mg/mL PEPC, 0.1 mg/mL MDH, 0.1 mg/ML carbonic anhydrase, 25mM phosphate buffer (pH 6.5), 0.5 mM $MgCl_2$, 5 mM PEP, 1 mM NADH, 5mM DTT and at 25°C. The 1x coupling enzyme mix contained PEPC, MDH and carbonic anhydrase, and the 2x buffer mix contained the co-substrates along with ferulic acid. The coupling enzyme mix and the buffer mix were added to a reaction well. Once the stable background reading of the change of NADH absorbance was observed, PAD enzyme was added to initiate the reaction.

2.2.4 $OleTJ_{JE}$ Expression and Purification

A wild-type $OleT_{JE}$ was codon-optimized and cloned into pET32a(+) vector via restriction cloning with BamH1 and Xho1 cut sites. The resulting plasmid was used to transform *E. coli* C41 (DE3). A 5 mL LB kanamycin culture was inoculated from a single colony and grown overnight at 37°C, shaking at 220 rpm. The overnight culture was used to inoculate a 500mL LB kanamycin culture and was grown at 37°C for 3-6 hours until an OD_{600} of between 0.4 and 0.6 is reached, shaking at 220 rpm. Once the correct OD was reached, 0.5mM IPTG and 0.5mM δ-aminolevulinic acid were added and the culture was placed in the shaker overnight at 18°C, shaking at 220 rpm. The cells were harvested by centrifugation using 450 ml centrifuge bottles and the JA-10 rotor (10,000×g; 15 minutes; 4°C). The cell pellet was resuspended in lysis buffer (50mM sodium phosphate, 300mM NaCl, 10mM imidazole, 10% glycerol at pH 8.0). Lysozyme,

DNAse I, and RNAse A were added each to a final concentration of 5 µg/mL and a Roche protease inhibitor cocktail was added to the cell suspension. The suspension was subsequently sonicated and then spun down using 50 mL centrifuge tubes and JA-30.50 rotor (15,000×g; 30 minutes; 4°C). The supernatant was filtered with a 0.22 µm syringe filter. The suspension was run through a 1ml Ni-NTA resin column to capture $OleT_{JE}$. The column was equilibrated with 10-15mL of wash buffer (50mM sodium phosphate, 300mM NaCl, 20mM imidazole, 10% glycerol pH 8.0). The suspension ran through the column and then the column was washed with 10-15mL of wash buffer. The elution buffer was added to the column with an Akta FPLC. The fractions containing eluted OleT were then collected and buffer exchanged and stored in storage buffer (100mM potassium phosphate (monobasic), 750mM NaCl, 20% glycerol pH 8.0).

2.2.5 Site-Directed Mutagenesis of $OleT_{JE}$

Wildtype $OleT_{JE}$ was mutated through PCR-directed site-specific mutagenesis with Phusion enzyme using a mutagenic sense (5' GGCGCGATTCAGACCGTTGATGG 3') and anti-sense 5' CCATCAACGGTCTGAATCGCGCC 3') primers. The PCR product was digested with Dpn1 at 37 °C for 1 hour, and then was run through a column from the Qiagen PCR Purification Kit. The purified PCR product was transformed into DH10B.

2.2.4 Determining Reinheitszahl (Rz) Ratio for P450

The Rz ratio is the ratio between the absorbance of heme (420nm) to protein (281nm). This is determined with a UV-absorbance 96 well plate to obtain an absorbance spectrum of the sample containing P450 $OleT_{JE}$ using a ClarioStar plate reader.

Chapter 3: Results and Discussion

3.1.1 Design of a PEPC-MDH Coupled Assay

To detect decarboxylase activity, we made use of coupling enzymes phosphoenolpyruvate carboxylase (PEPC) and malate dehydrogenase (MDH). In this *in vitro* assay, $OleT_{JE}$ catalyzes the decarboxylation of a fatty acid and produces a terminal alkene and CO_2. The released CO_2 is detected by the coupled reactions that ultimately result in the oxidation of NADH, which can be detected spectrophotometrically. Carbonic anhydrase converts CO_2 and water to bicarbonate, which subsequently reacts with phosphoenolpyruvate (PEP) to form oxaloacetate in a reaction catalyzed by PEPC. Oxaolacetate is then reduced in a reaction catalyzed by MDH that concurrently oxidizes a NADH co-factor to produce malate and NAD^+. Through the coupled reactions, released CO_2 from the enzyme-catalyzed reaction leads to a decrease in NADH concentration, which absorbs at 340 nm. NADH absorbance is used as a signal to detect the decarboxylation reaction catalyzed by the enzyme of interest.

Since the detection of decarboxylase activity is dependent on measurements of the change in NADH concentration, we determined the dynamic range for spectrophotometric quantitation of NADH by absorbance at 340 nm. We observed that the relationship between NADH absorbance and concentration is linear between 0-2 mM (**Figure 5A**). In the subsequent decarboxylase assays, we used a NADH concentration within this linear range to ensure accuracy in determining NADH concentration from NADH absorbance (at 340 nm), which then allows us to relate NADH absorbance to fatty acid decarboxylation. Essentially, 1 mol of CO_2 produced theoretically leads to 1 mol of NADH oxidized under ideal conditions. For the initial validation

of the assay, we began by testing the latter steps of the assay (after the production of bicarbonate) with a truncated version of our design using the coupled PEPC and MDH enzymes (**Figure 5B**).

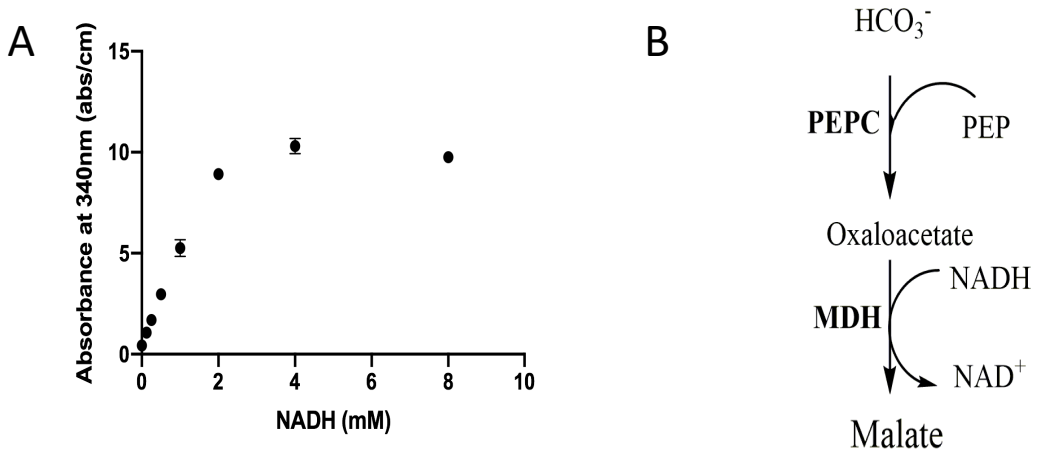

Figure 5. **The PEPC-MDH Reaction network and dynamic range of NADH** A) The PEPC-MDH assay scheme. PEPC catalyzes HCO3- and PEP to oxaloacetate. The MDH-catalyzed reaction leads to the oxidation of NADH to NAD^+. NADH can be detected at an absorbance of 340nm. B) From the NADH standard curve, a linear range between 0-2mM where a change in NADH concentration will correspond to a linear decrease in absorbance at 340nm.

In the truncated version of the assay, the aim was to show that in an assay environment exposed to atmospheric CO_2 (where gas is exchanged with the atmosphere), added $KHCO_3$ will elicit a greater response than the background, which is affected by atmospheric CO_2 . As shown in **Figure 6A**, we observed that after 14.5 mins without PEPC or MDH, the reaction did not lead to a decrease in NADH absorbance at 340 nm. However, with the coupled enzymes present there was an observable decrease in NADH absorbance. The greatest decrease in NADH absorbance was observed when $KHCO_3$ (1 mM) was included in the reaction. It was predicted that even with

no addition of $KHCO_3$, we would observe a decrease in absorbance at 340 nm resulting from the oxidation of NADH because at basic pH (pH 8) HCO_3^- is present. CO_2 from the atmosphere dissolves readily in water and is in equilibrium with HCO_3^-, at pH 8 the equilibrium favours HCO_3^- form. This validates the potential application of this assay as a fixed screen for improved decarboxylation reactions.

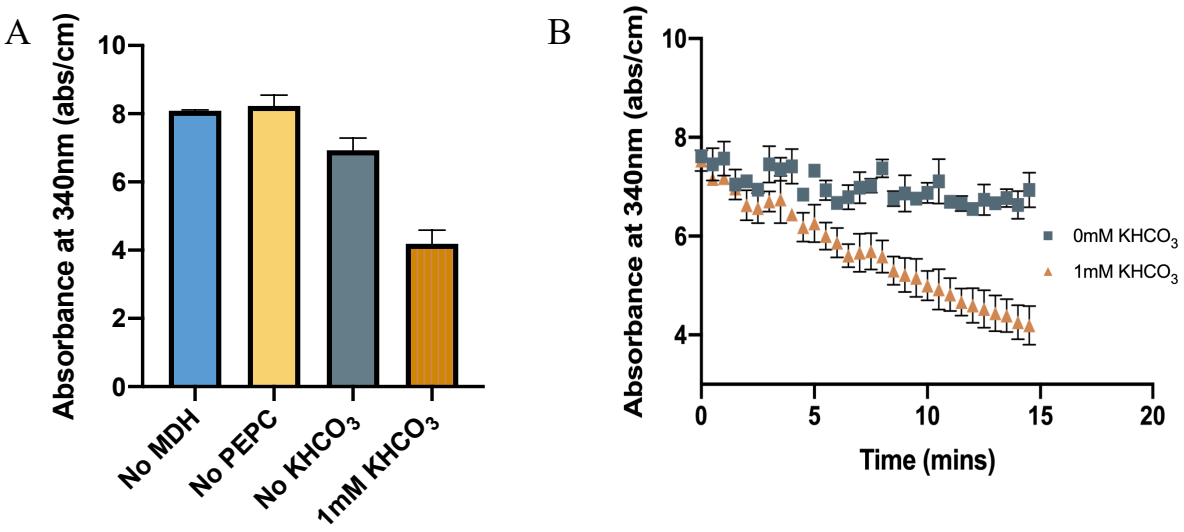

Figure 6. The PEPC-MDH Assay
A) Results of the PEPC-MDH reaction presented as a fixed-time point assay after 12mins of the PEPC-MDH assay in dupicate. B) The PEPC-MDH reaction presented as a continuous curve.

The PEPC-MDH assay can be also used as a continuous assay to show the decrease in NADH in a time-course (**Figure 6B**). NADH absorbance decrease can be observed as a linear rate in the presence of 2.5 mM $KHCO_3$. This suggests that the assay can be used to detect not only decarboxylation, but the rate of decarboxylation reactions given that they are rate-limiting among the coupled reactions. When using the full assay, other considerations need to be taken into

account such as differing pH, solvent and temperature conditions, as well as substrate, product or co-factor effects on the signal.

3.1.2 Optimization of PEPC-MDH Assay

The coupling enzyme system was observed to work under the initial testing conditions, but these may not have been the optimal conditions for the system. In this section, we detail the optimization of the latter part of the system that we devised to assay decarboxylase activity (consisting of the steps downstream of bicarbonate production—that is the reactions catalyzed by PEPC and MDH).

PEPC is an enzyme that catalyzes a two-substrate reaction, which consumes PEP and HCO_3^- to produce oxaloacetate and inorganic phosphate, and for the assay PEP concentration should be saturating (Bridger, Biochemistry, Alberta, & Tg, 1980). For the purposes of this assay, pseudo-first order kinetics must be observed for PEPC. To achieve this, saturated levels of PEP creates a rate of reaction dependent on $KHCO_3$ concentration. To identify PEP saturation levels, $KHCO_3$ was saturated and PEP concentration was varied. We observed that PEP was saturating at concentrations over 1.25 mM (**Figure 7**). The concentration of PEP required to reach 99% of Vmax, would need to be 20-fold higher than the K_m of PEP. For the purposes of this assay, we continued with 5 mM as our concentration of PEP; however to increase the rate of the rate of reaction and the sensitivity range of the reaction, higher levels of PEP can be employed.

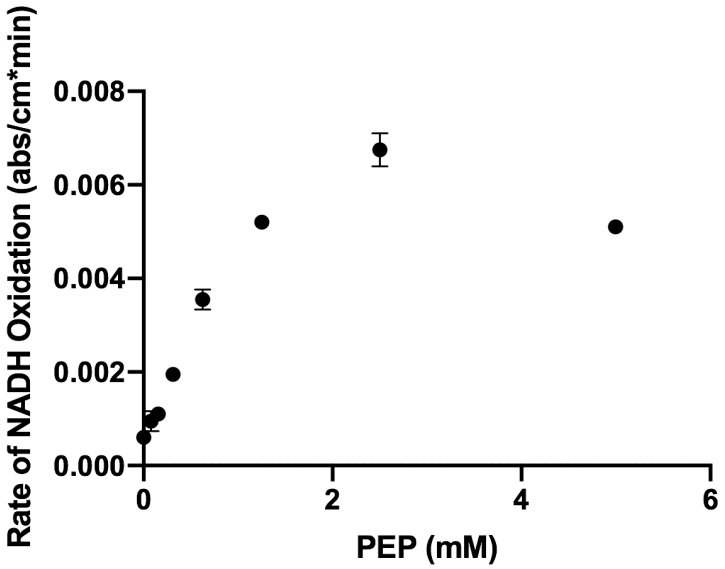

Figure 7. The optimization of PEP concentration in PEPC-MDH assay.
The PEPC-MDH assay with $KHCO_3$ as the saturated co-substrate (10mM) to identify concentration at which PEP is saturated (duplicates).

PEPC is a metalloenzyme that requires the co-factor Mg^{2+} which must be taken into account in the development of this assay (Bridger *et al*., 1980). Initially, with no Mg^{2+} added, the rate of NADH oxidation was low; however, upon addition of Mg^{2+}, the rate of reaction increased (data not shown). However, while the PEPC-MDH coupled reaction rate did increase, there was an increase in turbidity as $KHCO_3$ concentration was increased (**Figure A1**). $MgCO_3$ and $CaCO_3$ are common insoluble salts that are found in aqueous reactions, where CO_3^{2-} is in equilibrium with HCO_3^- (Mitchell, Jensen, Cliffe, & Maroto-Valer, 2010). In high enough concentrations of both ions, the salt will precipitate out due to its low solubility (Power, Harrison, Dipple, & Southam, 2013). The insoluble salt was detected by measuring the absorbance at 340nm and 600nm to detect the increased turbidity of the PEPC-MDH reaction with increasing $KHCO_3$ concentrations. As HCO_3^- levels increased, so did the turbidity (**Figure A1**). Lowering the Mg^{2+} concentration reduced precipitate in the reaction and did not interfere with NADH absorbance readings. Moving forward, we chose 0.5 mM $MgCl_2$ for our PEPC-MDH reactions; however, the

ideal Mg^{2+} concentration can be optimized since the $MgCO_3$ precipitate is dependent on substrate and Mg^{2+} concentration.

The limits of PEPC-MDH assay were analyzed to determine the concentration limits of our enzymes of interest. Detection limits for the assay dictate how the assay can be used and which enzymes can be used. If the K_m for an enzyme is lower than the detection limit, it cannot be used to determine the Michaelis-Menten kinetics. For Michaelis-Menten kinetics, substrate concentrations should be between 1/10 K_m and 10x K_m to obtain the Michaelis-Menten kinetic curve. The difficulty with the PEPC-MDH assay is the background noise that can affect the rates of the assay (Smithson *et al*., 2010). The limit of detection is dependent not only on the capacity of the PEPC-MDH assay to detect $CO_{2(aq)}$ or $HCO_3^-{}_{(aq)}$ in solution, but whether the assay can detect the difference between a given substrate concentration and background $CO_{2(aq)}$ and HCO_3^- in the solution to illicit a signal difference (Smithson *et al*., 2010).

Here, we observed the range of additional HCO_3^- that the assay can detect from the background (**Figure 8D**). We predict that as HCO_3^- concentration is increased, the difference will be greater. But for the purposes of the assay to detect Michaelis-Menten kinetics, we would need to see small signal difference between background and low signal concentration.

3.1.3 Considerations of Decarboxylation Assay

The observable difference between 0-150 μM $KHCO_3$ is low and quite noisy (**Figure 8A**). This indicates that for substrate ranges between 0-150 μM for the assay, under these conditions the results will be noisy as well.

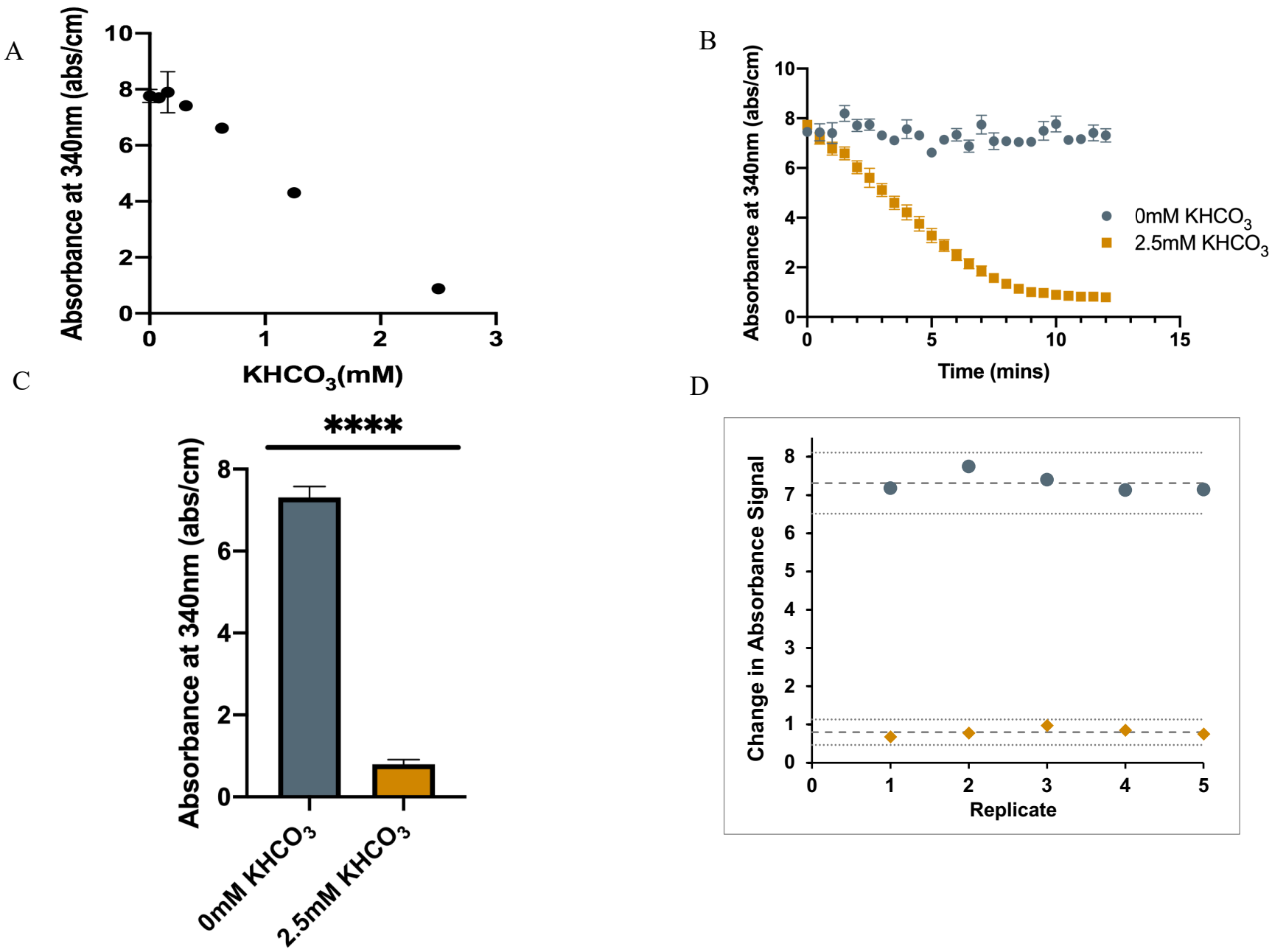

Figure 8. Decarboxylation assay.

A) The detection range of the PEPC-MDH assay to(duplicates). B) Repeated the PEPC-MDH assay with 5 replicates to observe the signal-noise ratio of the assay with higher concentrations of $KHCO_3$. C) The PEPC-MDH assay from A presented as a fixed-time point assay after 10mins (**** unpaired two-tail t-test, $p<0.0001$). D) With the 5 replicates, the Z' of the assay was calculated to be 0.83.

While the rate of reaction was optimized, background CO_2 was still a considerable concern since CO_2 is quite soluble in water. Previously, this assay developed by Smithson *et al*., was used in an anaerobic chamber where CO_2 was purged to reduce the background signal in solution (Smithson *et al*., 2010). We developed a protocol to use the assay and remove the background affect without an anaerobic chamber. Before the addition of our substrate, we let the PEPC-MDH reaction begin and consume the $CO_{2(aq)}$ initially dissolved in the system until the change in signal "levels off" before adding substrate of interest, enzyme or co-factor to trigger the decarboxylation reaction. What we describe as a "leveling off" is not a flat signal, but actually the observed small decrease of NADH measured spectrophotometrically due to oxidation (data not shown). We hypothesize that what we are observing is partitioning of $CO_{2(g)}$ from the atmosphere into the reaction mixture as dissolved $CO_{2(aq)}$, to which the coupled enzymes in our assay are sensitive. In atmospheric environments, CO_2 will always be a concern and should be taken into account in the assay. However, the aim is to improve the signal-noise ratio of the assay enough to detect decarboxylation.

With the decarboxylation method to reduce the background signal, we proceeded with the PEPC-MDH coupled assay and observed a significant difference in the signals between 0mM $KHCO_3$ and 2.5mM $KHCO_3$ (**Figure 8B**). The large difference in rate from the continuous curve between the control and added substrate, along with the end-point difference of the fixed assay is promising that the method was successful (**Figure 8C**). The reaction occurred in 5 replicates and with that we calculated a Z' of 0.83 (**Figure 8D**). The Z' describes the signal-noise ratio of an assay and for a high-throughput assay, the closer the Z' is to 1 the closer the assay is to being "ideal"

While background $CO_{2\,(aq)}$ can be reduced, it will continue to dissolve into the reaction system from the atmosphere. From our experiments, it can be observed that the negative controls (no added $KHCO_3$) still have a negative slope. The negative slope is due to background $CO_{2(aq)}$ in solution and NADH oxidation (Fernandes, Neto, Kubota, & Katekawa, 1998). When measuring the absorbance of NADH in buffered solutions, the absorbance of NADH may decrease and the rate of this decrease is a function of the pH and the buffer (Fernandes *et al*., 1998). Taking this into account, the decrease in absorbance from a NADH control dissolved in the same buffer as the reaction of interest is also measured and the negative rate is subtracted from measured rates in the assay.

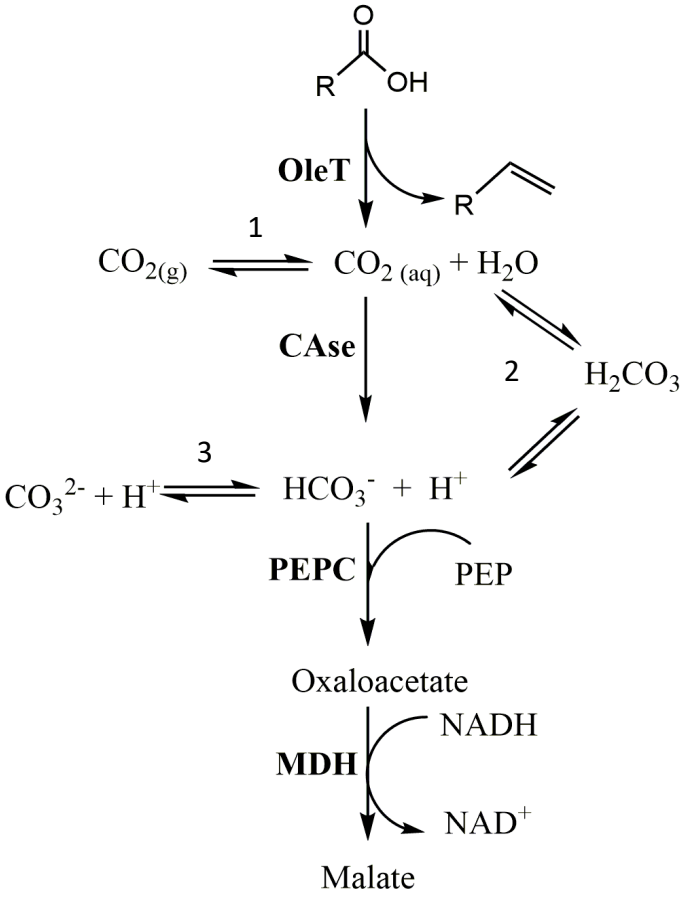

Figure 9. **The full reaction network of the OleT$_{JE}$ assay and the equilibria of $CO_{2(aq)}$.**
1) CO_2 is in equilibrium between its gaseous and dissolved state. 2) Carbonic acid is rapidly formed from $CO_{2(aq)}$ and H_2O, but quickly converts to HCO_3^-. 3) HCO_3^- is in equilibrium with CO_3^{2-}. CO_2, HCO_3^- and CO_3^{2-} are forms of the CO_2 equilibria in water.

$CO_{2(aq)}$ is in equilibrium with $CO_{2(g)}$ and diffuses out of water at a constant rate (**Figure 9**) (Mitchell *et al*., 2010; Power *et al*., 2013). $CO_{2(aq)}$ has multiple equilibrium forms and they must be taken into account when measuring $CO_{2(aq)}$. An attractive solution may be to subtract the observed linear net rate of $CO_{2(aq)}$ dissolving into the aqueous solution calculated from the control; however that would not be a perfect correction factor since some CO_2 is also lost to the atmosphere as previously stated, but some is also lost to the equilibria partners of $CO_{2(aq)}$. When CO_2 dissolves in water it is reacts with water to form, $H_2CO_{3(aq)}$. $H_2CO_{3(aq)}$ is subsequently in equilibrium with $HCO3^-$ and then CO_3^{2-} ions. As previously observed with the formation of $MgCO_{3(s)}$ in our assay, CO_2 equilibria exist in these forms. Upon the decrease of Mg^{2+} the precipitate had decreased; however, the carbonate ion is still present in the aqueous solution and is unobservable (**Figure A1**) (Mitchell *et al*., 2010; Power *et al*., 2013). If some of the reactants are lost to the CO_2 equilibria, it limits the applications of this assay. While the PEPC-MDH assay is a continuous assay and rates can be observed, the rates are not exact due to the loss of CO_2 in other forms. A promising method to more accurately detect V_{max} and K_{cat} with this method is to simulate the reaction and correct for the background reaction. There are numerous models of the behaviour of CO_2 and its equilibria in different conditions due to its interest in oceanic and atmospheric science (Eriksson & Welander, 1955; Misra & Verma, 2013; Mitchell *et al.*, 2010).

When used as an application to test the Michaelis-Menten kinetics of an enzyme, the assay can detect the K_m of the reaction since K_m is an independent value in the Michaelis-Menten curve. A rapid way of detecting K_m is still valuable in the characterization of enzymes, since the K_m can provide an insight into the substrate levels that will saturate the enzyme rate (such as the K_m of PEP and it's insight into saturating the rate of PEPC). In addition, the assay can function well as

a screen to compare activities between different reactants. So with this in mind, we move forward with applying the assay as a high-throughput screen for $OleT_{JE}$.

3.2.1 $OleT_{JE}$ Expression and Purification

Recombinant protein expression and purification from *E. coli* are well established for many proteins, however many proteins are difficult to express and conditions must be optimized. $OleT_{JE}$ gene was codon-optimized for *E. coli* and was cloned into pET28a(+). In initial expression attempts, $OleT_{JE}$ was transformed into BL21(DE3) and expressed under general protein purification protocols. Under these conditions, we observed expression of the enzyme; however, there was no activity under our assay. The Reinztmann ratio or Rz ratio is the absorbance of heme binding to a P450 to the absorbance of total protein in the solution where heme-bound complex when bound to oxygen absorbs at 418nm and the protein absorbs at 280nm (Barry & Challis, 2012). To observe heme-protein binding, the Rz ratio of OleT was measured using a UV-transparent microplate to determine absorbance of protein and heme. For active P450 enzymes, an Rz >0.5 is expected (Barry & Challis, 2012). Our initial protein purification conditions produced a low concentration of Rz ratio (**Figure 10A**).

Optimizing protein purification conditions can be a difficult task and there are a few methods to try and improve heme integration into the purification. We saw a slight increase in heme purification once we added the heme precursor, δ-aminolevulinic acid (data not shown). The media used in purification can be optimized to improve purification.

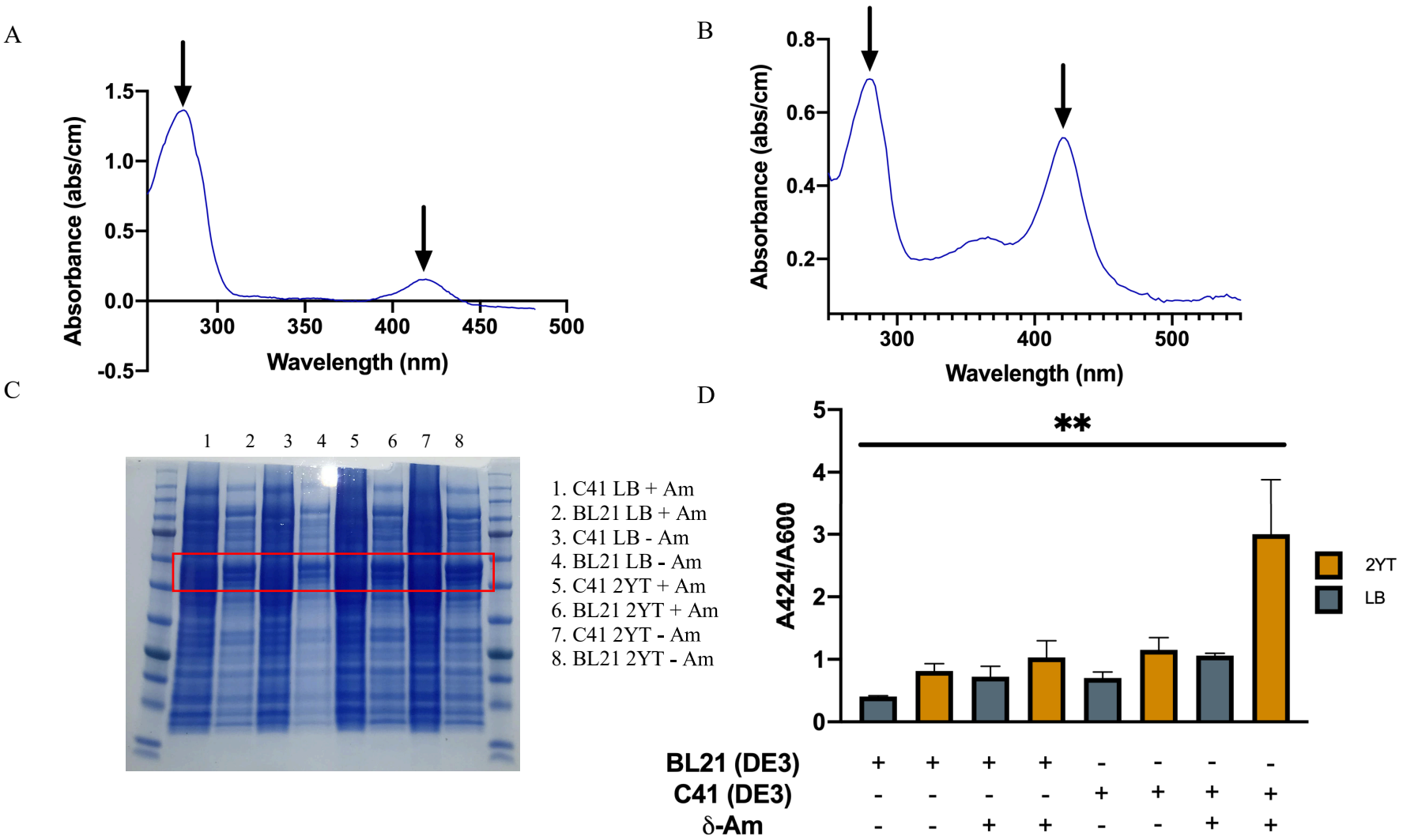

Figure 10. Optimization of $OleT_{JE}$ heme expression.

Absorbance spectra of $OleT_{JE}$ expression using A) BL21 (DE3) grown in LB media and B) C41 (DE3) grown in 2YT media. C) SDS PAGE of lysates from $OleT_{JE}$ Optimization. D) Normalized heme absorbance (peak at 424nm) of lysates under different growth conditions (** One-way Anova test, p=0.0015).

In literature, $OleT_{JE}$ was purified either in LB media or 2YT medium, where we found that 2YT was a better media for heme expression in $OleT_{JE}$ (**Figure 10B)**. Lastly, in literature, different strains have been used to express $OleT_{JE}$, BL21(DE3) and C41(DE3). C41 (DE3) is a BL21 derivative that is used to produce toxic and membrane proteins (Schlegel, Genevaux, & de Gier, 2017). Upon comparing the different conditions, we observed that expressing $OleT_{JE}$ in C41(DE3), 2YT and the heme precursor had the most optimal expression conditions. In fact, it seems combining all 3 conditions had a large improvement in heme incorporation and expression (**Figure 10D**).

2YT media contains twice the concentration of yeast extract and is often used in long growth conditions. The richness of the media could provide an explanation for higher expression of $OleT_{JE}$ with bound heme. The T7 promoter expression system is widely used to purify proteins.

BL21 (DE3) contains T7 RNA polymerase that is under the inducible lacUV5 promoter (Dumon-Seignovert *et al*, 2004). C41 (DE3) was discovered after BL21 (DE3) was transformed with a toxic protein and the mutants that survived were selected and identified (Dumon-Seignovert *et al*, 2004). C41 (DE3) has mutations that allow the strain to better handle toxic proteins and stress compared to BL21 (DE3). Specifically, C41(DE3) contains a mutant weak lacUV5 promoter where proteins are expressed at a slower rate (Dumon-Seignovert *et al*, 2004). These conditions may explain the improved $OleT_{JE}$ expression.

3.2.3 Optimization of $OleT_{JE}$ Assay

To further build on the PEPC-MDH coupled assay, $OleT_{JE}$ and carbonic anhydrase have been added to identify whether carbonic anhydrase can increase the rate of reaction and more rapidly detect an increase in CO_2 concentration leading to a decrease in NADH absorbance. When CO_2 is dissolved in water, it reacts with water to form carbonic acid, H_2CO_3. Dissolved CO_2 and H_2CO_3 have an equilibrium at near neutral pH, but the uncatalyzed interconversion between the two is very slow. Carbonic anhydrase catalyses this reaction but significantly faster than the non-catalyzed reaction.

In **Figure A3**, there was a slight observable decrease in NADH absorbance where carbonic anhydrase was not present. We did observe a notable difference between presence of fatty acid and no fatty acid, which is promising (**Figure A3**). There is a significant difference in the rate of reaction between the conditions where carbonic anhydrase was absent and carbonic anhydrase was present. This strongly suggests us that upon decarboxylation, $OleT_{JE}$ releases CO_2 as a product (and not HCO_3^-). Previously, the PEPC-MDH and carbonic anhydrase have been coupled to determine the CO_2 equilibrium product from a decarboxylase (Liu *et al.*, 2001; Witkowski, Joshi, & Smith, 2002). The decrease in NADH absorbance in the presence of carbonic anhydrase, reveals that without carbonic anhydrase, the PEPC-MDH coupled assay will not be able to detect $OleT_{JE}$ activity. All iterations of the assay below will use PEPC, MDH and carbonic anhydrase to detect decarboxylase activity (**Figure 11**).

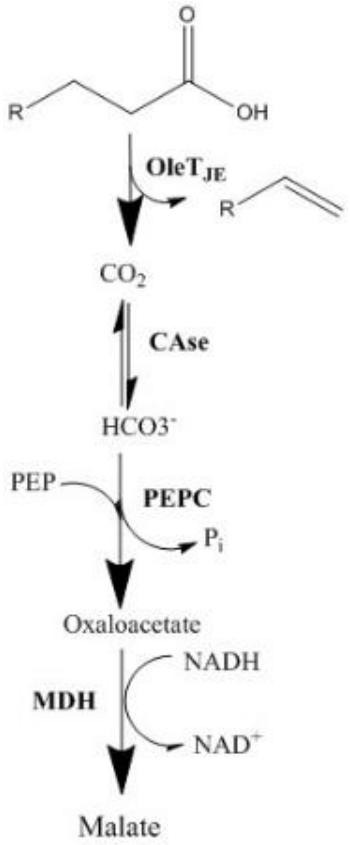

Figure 11. The full scheme of the PEPC-MDH assay with OleT$_{JE}$ and carbonic anhydrase.
In this scheme, 1 mol of CO_2 released from the decarboxylation reaction will lead to 1 mol of NADH oxidized.

$OleT_{JE}$ is a peroxygenase, which is an important point of optimization when H_2O_2 is a powerful oxidant that can interfere with multiple enzymatic processes. For the purposes of this assay, since the reaction cannot occur without the presence of the catalyst H_2O_2, it can be used as a method to trigger the reaction. It was previously reported that a final solvent mixture of 10% DMSO would improve $OleT_{JE}$ rate of reaction (Bojarra, Reichert, & Grote, 2018). We confirmed that a 10% DMSO mixture would improve the rate of reaction and does not seem to directly impact the PEPC-MDH assay (data not shown). H_2O_2 also was able to trigger the $OleT_{JE}$ reaction, which can be a step to begin the reaction in future high-throughput applications (**Figure A4**).

3.2.4 OleT$_{JE}$ Assay for Screening

With the optimized conditions, we ran the OleT$_{JE}$ assay, which consists of the all the optimized components and conditions. With all of the optimized conditions, we observe that there is a significant signal difference when enzyme is present and when it is not (**Figure 12**). In future analysis of different fatty acid decarboxylases or mutant OleT$_{JE}$, this screen can potentially be used as a comparative method exists to study their behaviour. Moving forward, this reaction condition is what is used to further study OleT$_{JE}$.

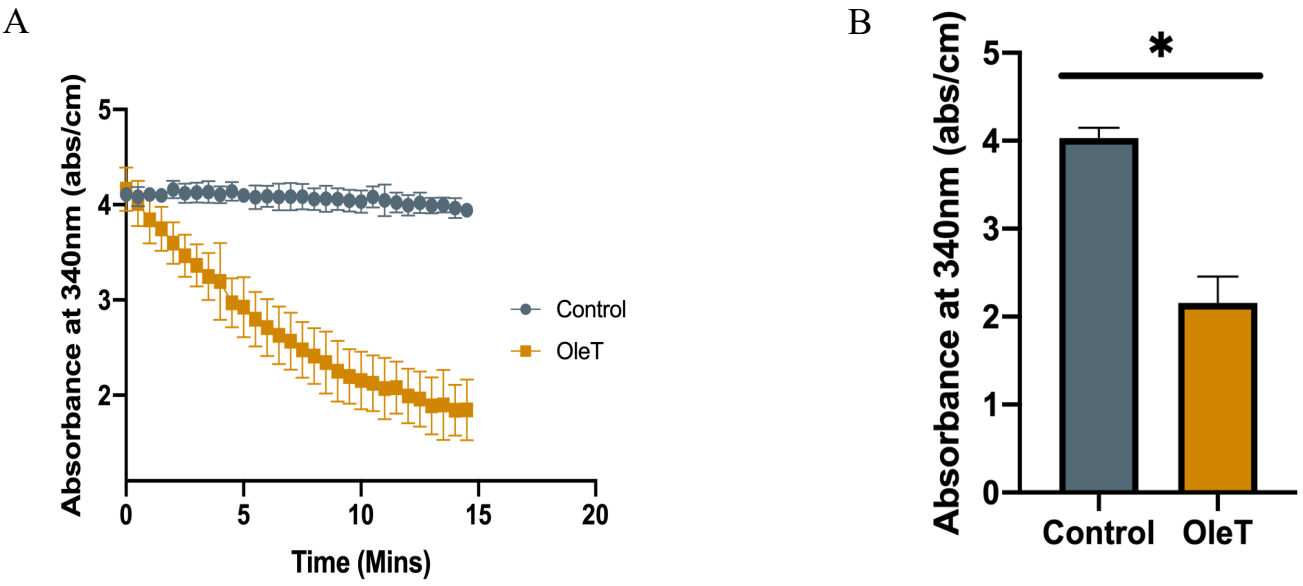

Figure 12. The OleT$_{JE}$ Assay.
OleT Screen in the presence or absence of OleT$_{JE}$ A) Continuous curve and B) End point at 10mins (* unpaired two-tail t-test, p=0.0146 [duplicate]).

For a brief analysis of OleT$_{JE}$ as a method to screen activity against different fatty acids, myristic acid (C14), arachidic acid (C20) and stearic acid (C18) were screened with the assay to detect differences in end-point values (**Figure A5**). It has been reported that OleT$_{JE}$ has different

product yields for the different fatty acids (Matthews *et al*., 2017). The different end points can be noted in the reaction, providing more insight into $OleT_{JE}$ activity and functionality, as well as utility of the proposed assay.

The rate of enzyme catalysis is dependent on substrate binding specificity and the catalysis of the reaction which is also substrate dependent. It would be expected that for different fatty acids would then also have different rates of reactions and differing endpoints. The closely parallel rates suggests that in this coupled assay, another enzyme is the limiting enzyme in the reaction. $OleT_{JE}$ was added in excess for the purposes of this test and for more accurate results around end points and differing rates, $OleT_{JE}$ should be the limiting enzyme in the reaction. However, the test showed us that different fatty acid substrates can illicit a signal difference from the negative control. For future applications with limiting $OleT_{JE}$, the assay can potentially be used to screen different substrates to detect differing decarboxylation activity.

3.2.5 Mutagenesis of $OleT_{JE}$

Some mutagenic studies for $OleT_{JE}$ have been carried out to characterize the enzyme's behaviour; however, the studies have been limited due to the low-throughput of GC/MS used in these studies. In these mutagenic studies, researchers have tried to elucidate the decarboxylation mechanism of $OleT_{JE}$, the only decarboxylases in the hydroxylase family of CYP152. Comparing the active site region of $OleT_{JE}$ to other fatty acid hydroxylase family members, there is an observable difference with one residue, a histidine at position 85 (Belcher *et al*., 2014). $OleT_{JE}$ and related decarboxylase enzymes in this protein family consistently contain this residue in the active site, while instead a glutamine is conserved near the heme in fatty acid

hydroxylases. Glutamine is a conserved amino acid in this position and the only noticeable difference in the residues of the CYP152 class family and $OleT_{JE}$ from aligning the sequences indicates that the residue might trigger decarboxylation (Rude *et al*., 2011). $P450_{\beta S\beta}$ a well-known member of the CYP152 family, had the glutamine residue mutated to histidine and decarboxylated products were produced in low concentrations (Rude *et al*., 2011). This further suggests that the mutation may be key in the catalytic mechanism of $OleT_{JE}$ decarboxylation.

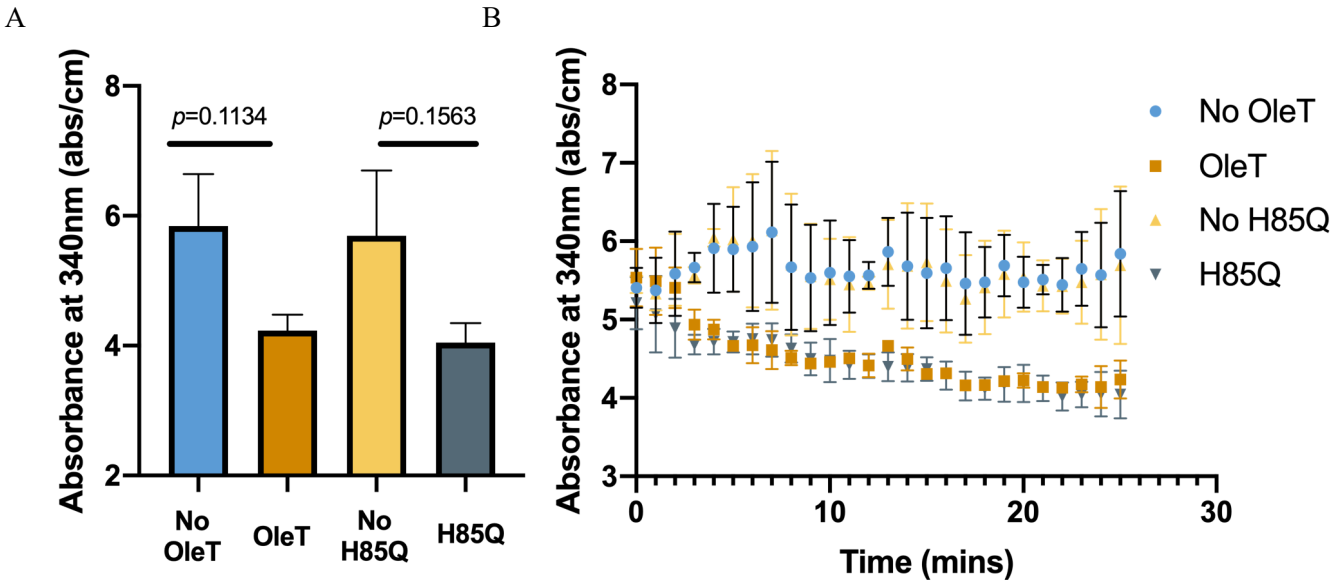

Figure 13. The $OleT_{JE}$ H85Q Mutant Screen
OleT assay to test the activity of the wildtype OleT and H85Q mutant for 250 µM Myristic Acid. A) Endpoint after 25mins (unpaired two-tailed t-tests) B) Continuous curve of reaction (duplicate).

We mutated the $OleT_{JE}$ active site from histidine to glutamine using site-directed mutagenesis, to observe the effect on catalytic activity. It was predicted that the mutation would reduce or nullify decarboxylase activity, since it is the residue difference in the conserved reside of the

hydroxylase family. Upon confirming the correct mutation with sequencing, we screened for activity of the mutant compared to the wildtype.

The presence of either wildtype $OleT_{JE}$ or the H85Q mutant appeared to lead to a decrease in signal in the PEPC-MDH assay, but there is considerable error in measurements using substrates in the micromolar range (**Figure 13A**). The signal decrease in the H85Q mutant suggests that H85Q mutant is still an active decarboxylase, which we confirmed with GC/MS (data not shown). Two different research groups reported two opposing effects of a H85Q mutation where one group found that the H85Q mutant was still active and another found that it had lost activity (and by active it is meant that H85Q favours decarboxylation over hydroxylation) (Fang *et al*., 2017; Matthews *et al*., 2017). The results we obtained inform us that it is more likely that the H85Q mutant creates a decarboxylated product, validating the results from Matthews *et al* (Matthews *et al*., 2017). The curves of the $OleT_{JE}$ wildtype and mutant are highly similar, may indicate that the $OleT_{JE}$ enzymes are not the limiting enzyme in the reaction itself. However, in literature Matthews *et al* observed that H85Q and wildtype $OleT_{JE}$ have very similar product yields and activity (Matthews *et al*., 2017). Here, we see that the activity of $OleT_{JE}$ and its variant can be detected with this developed assay. We created a mutant of $OleT_{JE}$ and were able to detect the decarboxylation reaction which is promising for future applications of the assay.

The assay must be further optimized as previously stated to gain more accurate results in the analysis of the screen. The ultimate goal with this screen is to study a large mutant library of $OleT_{JE}$ to improve its activity to make potential 'drop-in' biofuels. For this to occur, there are many considerations in the optimization of the assay, such as the effect of lysate conditions on the assay, the expression strain, background NADH signal from lysate will need to be

determined. As a continuous curve, the PEPC-MDH assay appears detect the rate of reaction of $OleT_{JE}$ and the H85Q mutant (**Figure 13B**). Determining the Michaelis-Menten kinetics of $OleT_{JE}$ with GC/MS takes an exceptionally longer time than the continuous spectrophotometric assay, which is more rapid and efficient than a GC/MS-based assay.

3.2.6 Michaelis-Menten Kinetics of $OleT_{JE}$

As stated in the previous section, the assay contains carbonic anhydrase, PEPC and MDH enzymes that all have rates of reactions. For Michaelis-Menten kinetics, it is important for $OleT_{JE}$ to be the limiting enzyme in its rate of reaction, otherwise the rate of decrease of NADH absorbance or NADH oxidation will be due to another enzyme in the system, the limiting one. In this range, the rate of reaction is dependent on the concentration of $OleT_{JE}$, not the other coupling enzymes. The dynamic range where $OleT_{JE}$ will be the limiting enzyme will present as a linear segment of the curve plotted from the the Rate of Reaction vs Enzyme concentration. The linear range indicates that the rate of reaction is dependent on the subsequent increase or decrease of $OleT_{JE}$ in a linear manner. When $OleT_{JE}$ concentration is high and the decarboxylation reaction no longer rate-limiting, the rate of the coupled NADH oxidation (measured by absorbance) reaches a plateau and does not change when $OleT_{JE}$ concentration changes. At this point, one of the other coupling enzymes catalyzes the rate-limiting reaction in the coupled assay. The linear range indicated in **Figure 14A**, is where the concentration of $OleT_{JE}$ used in the Michaelis-Menten Kinetics was chosen.

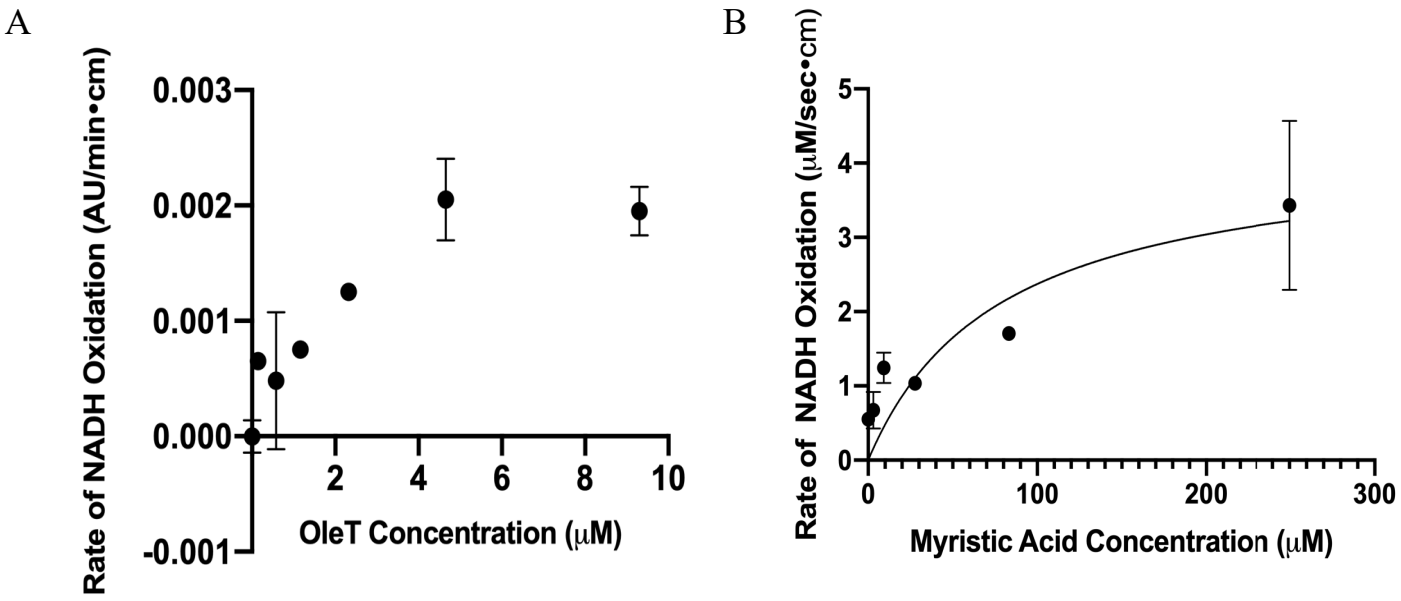

Figure 14. $OleT_{JE}$ enzyme kinetics.
A) The observed rate of NADH change in absorbance against varying concentrations of $OleT_{JE}$. B) The Michaelis-Menten curve of $OleT_{JE}$ with the PEPC-MDH assay using fluorescence as the method of detection.

In the PEPC-MDH assay, NADH is detected by its absorbance at 340nm. However, NADH can also be observed under fluorescence (Napper & Sivendran, 2011). Fluorescence is an attractive method of detecting $OleT_{JE}$ activity since it is significantly more sensitive than absorbance. It also directly detects the molecule of interest, while absorbance looks at the difference in light before and after light has passed through (Lakowicz & Lakowicz, 1999). The turbidity of a reaction can adversely affect the absorbance, while fluorescence is not impacted. The sensitivity of fluorescence also can lead to lower detection limits and less volumes of a reaction which is attractive in future applications of the assay to large mutant libraries. It can lower the cost of the assay and more importantly can be applied to libraries with low protein expression conditions. With these reasons in mind, we compared the detection of the reaction between fluorescence and absorbance. The results show that the decrease of NADH using absorbance and fluorescence had similar trends and that the there's an observable difference between the rates of the positive and

negative controls (**Figure A6**). The reported Km of $OleT_{JE}$ is ~ 24uM, which is a relatively small value and the sensitivity of fluorescence may aid in more accurately detecting $OleT_{JE}$ activity (Fang *et al*., 2017). With this in mind, we used fluorescence to detect the rates and subsequently the Michaelis Menten curve.

We identified the range where $OleT_{JE}$ is the limiting enzyme and used a concentration in the linear range to determine its' kinetics. Here, myristic acid was chosen to compare the results against literature since it is the only substrate where kinetic data of $OleT_{JE}$ was determined via GC/MS (Fang *et al*., 2017) . In **Figure 14B**, a Michaelis-Menten curve is plotted and the K_{mapp} determined via the assay was 78.3 ± 53.44 μM while the K_m from Fang *et al*, was reported to be 24 μM (Fang *et al*., 2017). The reported K_{mapp} from this assay is in agreement to the reported value in literature and is within the same order of magnitude. While the rate of reaction in the first few substrate concentrations generally lead to an upward trend, there was noise in the kinetic data as indicated by the standard error of the K_{mapp}. We observed that under the conditions of the assay between 0 – 150 μM of substrate is noisy and outside of the range of sensitivity (**Figure 8A**).

If the K_m for an enzyme is lower than the detection limit of an assay, the assay cannot be used to accurately determine the Michaelis-Menten kinetics. The difficulty with the PEPC-MDH assay is the background noise that can affect the rates of the assay. However, preliminary results have shown that increasing PEPC and MDH concentration in the assay, had led to an improvement on the detection range of the assay (**Figure A7**).

When used as an application to test the Michaelis-Menten kinetics of an enzyme, the assay can detect the K_m of the reaction since K_m is an independent value in the Michaelis-Menten curve. A rapid way of detecting K_m is still valuable in the characterization of enzymes, since the K_m can provide an insight into the substrate levels that will saturate the enzyme rate (such as the K_m of PEP and it's insight into saturating the PEPC rate). In addition, the assay can function relatively well as a screen to compare activities between different reactants, in the assay. With this in mind, we move forward with applying the assay to a non-P450, co-factor free decarboxylase.

3.3.1 Optimization of Assay to Sinapic Acid Decarboxylase (SAD) Enzyme

SAD was engineered from wild-type phenolic acid decarboxylase (PAD) derived from *Bacillus pumilus*, to expand its substrate scope and produce canolol, a powerful antioxidant, anti-inflammatory, and anti-carcinogenic (Morley, Grosse, Leisch, & Lau, 2013). PAD enzymes have diverse mechanisms and wide-importance in many industries; however, current methods are low-throughput (Kourist *et al*., 2014; Matte & Grosse, 2010; Morley *et al*., 2013). Here, we used SAD enzyme to showcase how the PEPC-MDH assay can be applied to PAD enzymes to optimize the engineering of this diverse group of enzymes.

The PEPC-MDH assay successfully detected the activity of wild-type OleT, a mutant of OleT and different substrates of OleT. The assay was optimized to be used for OleT and to be used for any other decarboxylase it must also go through a step-by-step optimization process. There are two points to note in the optimization of the assay for SAD. DTT, a reducing agent, is an important reactant in the SAD reaction it improves the rate of reaction and SAD is optimal at acidic pH conditions (Morley *et al*., 2013). However, for the purposes of our reaction we used pH 6.5 to test the activity of SAD. We observed that under these above conditions, the truncated

version of the PEPC-MDH assay functioned as expected and the decrease in NADH absorbance was linked to increasing $KHCO_3$ concentration (data not shown). With the functioning truncated assay under these two conditions, we tested the full assay.

When we first attempted the assay, there was no decrease of NADH observed by spectrophotometric measurement at 340 nM. Not observing a decrease in NADH absorbance, indicates that either SAD did not catalyse the decarboxylation of its substrate or that the assay could not detect the activity. If the enzyme was not functional, a decrease in NADH absorbance signal was expected. We measured the absorbance spectrum of ferulic acid, the substrate and observed that at 340nm it can interfere with NADH absorbance (**Figure 15**).

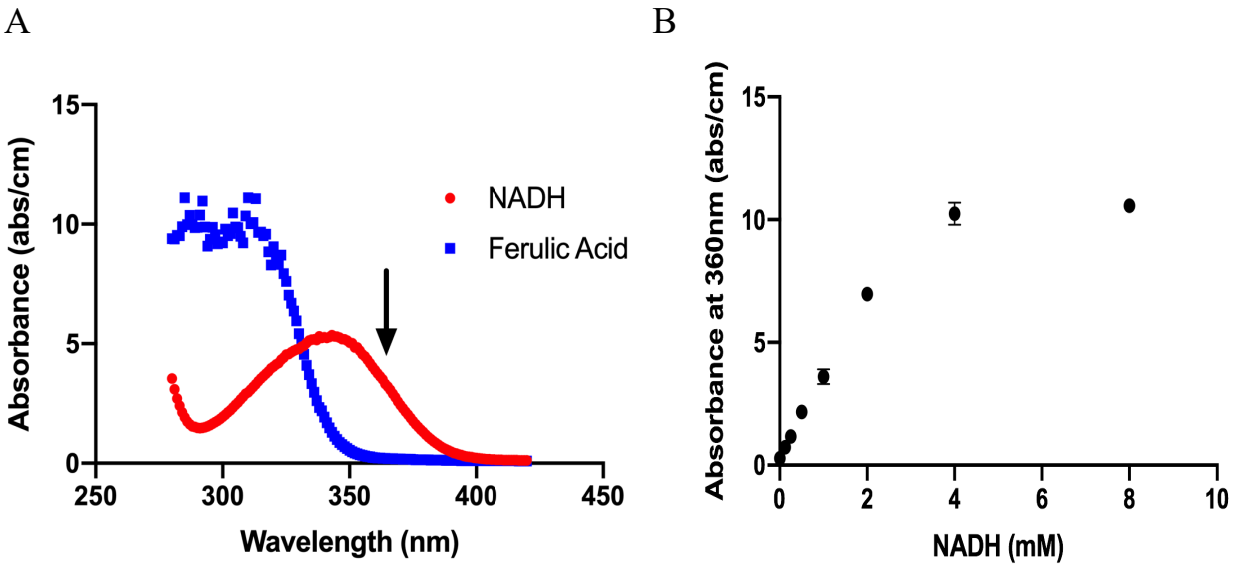

Figure 15. SAD Assay Optimization
A) Absorbance spectra of ferulic acid and NADH. The black dashed line is the NADH maxima at 340nm and the red dashed line is the absorbance being used to study SAD reaction with PEPC-MDH. B) Standard curve of the absorbance of NADH at 360nm at 25 ºC (duplicate).

At 360nm NADH absorbance is observable and Ferulic acid absorbance does not interfere with the readings. A linear region was observed on the standard curve of NADH at 360nm at 25 °C. This informs us that a decrease in NADH absorbance in the linear region can be linked to a change in substrate concentration. Moving forward 360nm was the absorbance used to observe NADH activity. The methods shown in Chapter 3.2 and in this section detail how to optimize this assay for future applications in decarboxylase methods. The versatility of the assay provides a framework to test different decarboxylases and how to optimize the assay for their conditions.

3.3.2 Application of PEPC-MDH Assay to SAD Enzyme

Here we applied the PEPC-MDH assay to analyze the detected rate of reaction catalyzed by SAD. The assay was applied to see whether the reaction has the ability of detecting the difference between substrate added and the absence of substrate. There was a significant signal difference between the absence and presence of substrate. This indicates that the assay was able to detect a difference between 0mM ferulic acid and 1mM ferulic acid (**Figure 16**).

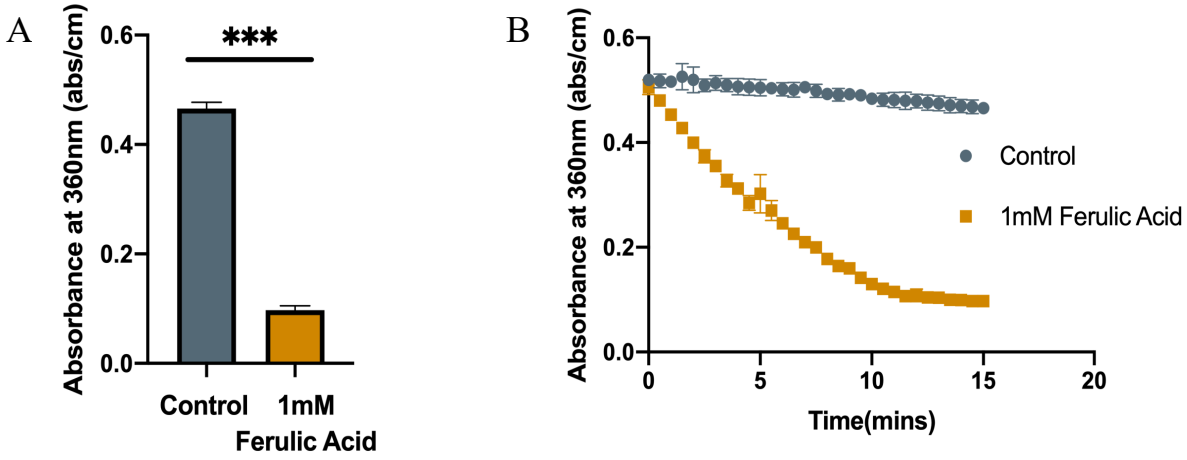

Figure 16. The SAD Assay
The PEPC-MDH assay with SAD enzyme to detect decarboxylation of substrate. A) End point after 15mins (*** unpaired two-tail t-test, p=0.007) and B) the continuous curve of the reaction (duplicate).

The assay can be used as a discrete fixed assay in this case. Since it is a plate-based assay, the assay can be adapted for high-throughput testing and provides a more rapid way of testing activity of SAD or other related phenolic acid decarboxylases with similar mechanisms.

Our assay can be used for further mutagenic studies of other phenolic acid decarboxylases. The mutagenesis studies can lead to further characterization of the decarboxylation mechanisms and to improve activity for these highly valuable products. The β-tunnel surrounding the active site, has already been mutated by Morley *et al* to expand the substrate scope of SAD and other phenolic acid decarboxylases (Morley *et al*., 2013). Future work in mutating the B-tunnel could expand the substrate specificity further and lead to promising method of highly sought out aromatic products (Morley *et al*., 2013). This is work our group is currently engaged with to characterize phenolic acid decarboxylase activity and mechanisms.

Since the assay is also a continuous assay, we were able to see a difference between the rates in the absence and presence of substrate. While there is a small negative rate in the slope in the absence of substrate, it is expected to behave this way since CO_2 still dissolves into the system at a set rate. However, for the purposes of this application, the difference between the rates is great enough to use the assay to study the behaviour of the SAD enzyme in a comparative fashion.

3.3.3 Michaelis Menten Kinetics of SAD

The experimentation in Section 3.3.3 was conducted by Dr. David Kwan and Jama Hagi-Yusuf

The substrate and products of SAD enzyme are detected and observed via liquid chromatography (LC) methods (Morley *et al*., 2013). Testing behaviour that is dependent on time with a fixed-point method, such as the kinetics of SAD, can be difficult and tedious to observe under these conditions. With the PEPC-MDH assay, the kinetics of SAD can be elucidated in a more efficient and rapid method.

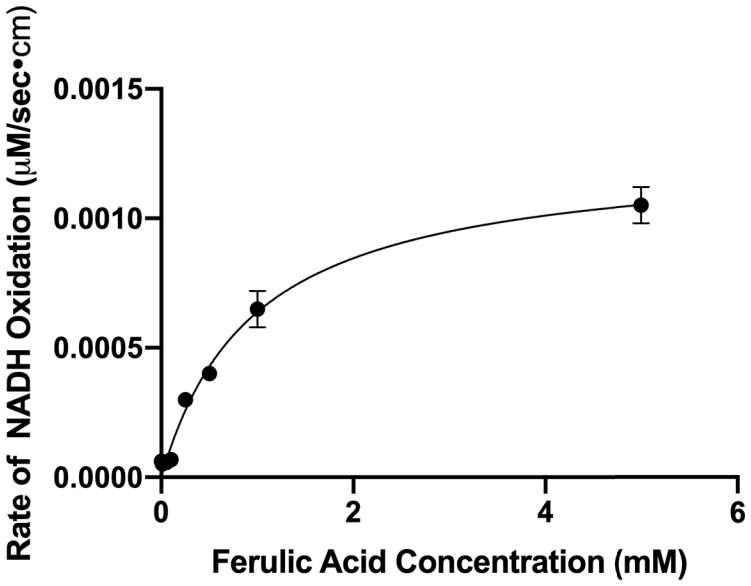

Figure 17. SAD enzyme kinetics
The Michaelis-Menten curve for SAD enzyme obtained from the PEPC-MDH assay (duplicates).

As a continuous assay, it can run multiple substrate conditions in parallel and the change in NADH absorption can inform in real-time the behaviour of an enzyme. Before beginning the reaction, similarly to $OleT_{JE}$ we must identify the region whereby SAD is the limiting enzyme in the reaction (**Figure A7**). Once identified, a concentration in this region was chosen to conduct

the assay to move the reaction forward. We ran 8 different concentrations of ferulic acid and observed the Michaelis-Menten curve for SAD. The K_{mapp} for ferulic acid was calculated to be 967.4 μM ± 108.6 μM, which is close to the reported Km in literature, 3.2mM (**Figure 17**) (Morley et al., 2013). The difference can also be due to pH differences, we tested the reaction at pH 6.5 and literature conducted the reaction at pH 7.0 (Morley *et al*., 2013).

The PEPC-MDH assay is capable of detecting the Michaelis constant for a phenolic acid decarboxylase enzyme. The assay can be used to detect the Michaelis constant for other substrates of SAD and other members of the phenolic acid decarboxylase family. Identifying the K_m for the substrates of SAD will enable researchers to understand the kinetics of the enzyme, but also enable further engineering of the enzyme for biotechnology applications. SAD was mutated to widen the activity of the enzyme for sinapic acid, a higher turnover for SAD can improve its capacity to be used as a biocatalysis in the production of canolol (Morley *et al*., 2013). While determining the higher turnover might not be accurate with our assay (as discussed in chapter 4), however it can provide a more rapid way to screen large libraries of decarboxylases that can then be more accurately tested and characterized with LC-MS methods. Applying this method can actively reduce the time to screen a mutant library or library of enzymes, in creating biorenewables.

Chapter 4: Concluding Remarks

We successfully adapted the PEPC-MDH coupled assay to detect the activity of $OleT_{JE}$, the activity of a mutant of $OleT_{JE}$ and a non-P450 decarboxylase, SAD. Here we also successfully showcased a method of optimizing not only the enzymes in this study, but other decarboxylases for our adapted assay. A generalizable high-throughput method for this class of enzymes is attractive for ease of use, rapid testing and adaptability for differing reaction conditions.

With this proof-of-concept, we can adapt the assay further for high-throughput conditions. Smithson *et al*, already showcased that these coupling enzymes can be used in a high-throughput manner (Smithson, *et al*., 2010). Many of the applications of the PEPC-MDH assay for high-throughput screening have been to detect inhibitors activities (Liao *et al*., 2015; Smithson *et al*., 2010).The reasoning may be due to the difficulty that may come with testing a mutant library. For future applications of $OleT_{JE}$ with a mutant library there are multiple considerations to undertake such as the strain, background from the lysate and the effect on the assay components.

Some of these considerations have already been taken into account in the development of a photoclick-based high-throughput assay and a colorimetric high-throughput assay for $OleT_{JE}$ (Markel *et al*., 2020; Xu *et al*., 2020). The photoclick-based screen was developed to detect higher activities of styrenyl decarboxylated products and the colorimetric screens for increased enzyme activity by observing H_2O_2 consumption in the reaction (Markel *et al*., 2020; Xu *et al*., 2020). These high-throughput screens are advantageous and can be used alongside the PEPC-MDH assay in characterizing $OleT_{JE}$. The PEPC-MDH assay can, in theory, screen for $OleT_{JE}$

activity of aromatic and non-aromatic substrates and is specific to decarboxylation reactions. H_2O_2 is a catalyst for the decarboxylation and hydroxylation reactions of $OleT_{JE}$ (Belcher *et al*., 2014; Rude *et al*., 2011). Our developed assay can be used to ensure the identification of high activity decarboxylation among the mutants screened by the high-throughput colorimetric assay.

Many of the mutations identified from the highest active mutant in the error prone mutant library of $OleT_{JE}$ by Xu *et al*., were found to be in the outer region of the enzyme (Xu *et al*., 2020). Mutagenesis of the active site of $OleT_{JE}$ has been limited, since changes to the region have led to decreased or neutral decarboxylation activity (Fang *et al*., 2017; Matthews *et al*., 2017; Rude *et al*., 2011). Mutating the hydrophobic pocket might pose a more interesting route to better widen or minimize the substrate specificity of $OleT_{JE}$. Belcher *et al* identified 3 residues at the entrance of the $OleT_{JE}$ hydrophobic pocket that evolved to expand its specificity to C20, compared to C16 for $P40_{BSB}$ (Belcher *et al*., 2014). Modulating the specificity of $OleT_{JE}$ binding to restrict the substrates capable of entering the pocket would provide a method of forcing $OleT_{JE}$ to favour medium chain length fatty acids which can lead to produce alkene products valuable in biofuels. Our assay can easily be adapted to study the difference in substrate specificities of a library of $OleT_{JE}$. The ability to screen and test different substrates of $OleT_{JE}$ and mutants of the enzyme will push a greater understanding of the enzymes' behaviour and catalytic mechanisms.

The successful detection of H85Q provides an insight that the assay can be used to screen different mutants studying the catalytic mechanisms $OleT_{JE}$. A limiting factor in the study of $OleT_{JE}$ is the low-throughput method of testing. Similarly to $OleT_{JE}$, SAD activity can be tedious to determine using a discrete testing system such as LC/MS.

The assay we developed showed that the SAD enzyme can be readily detected with a good signal-noise ratio. The K_m value observed is within the range of the PEPC-MDH assays sensitivity range. Future applications of SAD can be used to continue the work of Morley *et al* and expand the substrate scope of PAD class of enzymes (Morley, *et al*. 2013). We have begun testing mutants of SAD to assist our collaborators in Université Laval to further characterize the enzyme.

The defunctionalization of hydrocarbons that decarboxylases catalyze make them a powerful enzyme catalyst (Li, Huo, Pulley, & Liu, 2012). A greater understanding of their diverse mechanisms and behaviour can be valuable in the fine chemicals industry. Our developed high-throughput assay and the method to optimize the assay for the decarboxylases, provides a framework to further understand these mechanisms and apply them for biotechnological purposes. $OleT_{JE}$ terminal alkene products have the potential to push the energy industry into cleaner and more sustainable resources.

In accordance with the signed Paris Agreement, Canada aims to keep global temperature levels from pre-industrial revolution to 1.5 °C – 2 °C (Bush & Flato, 2019). By increasing the use of biofuels to 10-15% of fuel resources by 2030, greenhouse gas emissions would be reduced by 15 million tonnes each year (Clean Fuel Steering Committee, 2019). In Canada, the mean temperature has increased by 1.7 °C in Canada and 2.3 °C in Northern Canada (Bush & Flato, 2019). While the devastation of climate change has Cleaner fuel sources will not fix the effects

of climate change but will minimize them. The Canadian government and the rest of the world will need to implement a multipronged strategy to safeguard the planet.

Appendix A: Supplementary Results and Figures

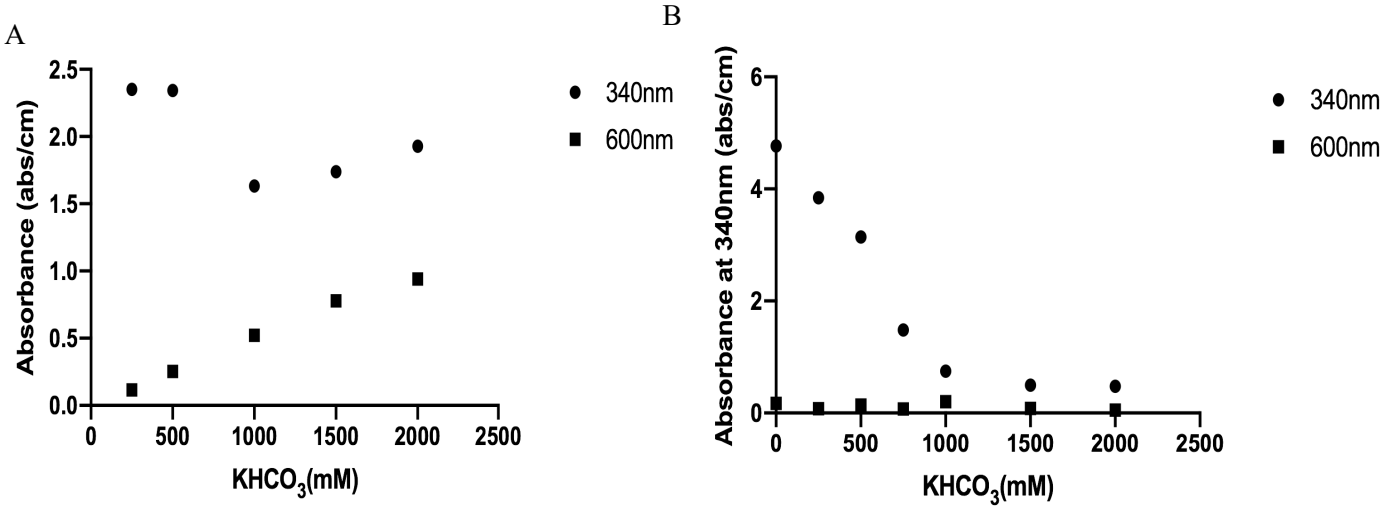

Figure A1. The effect of $MgCl_2$ concentration on Turbidity.
Testing the effect of two different $MgCl_2$ concentrations in PEPC-MDH Assay A) 2 mM $MgCl_2$ and B) 0.5mM $MgCl_2$

A

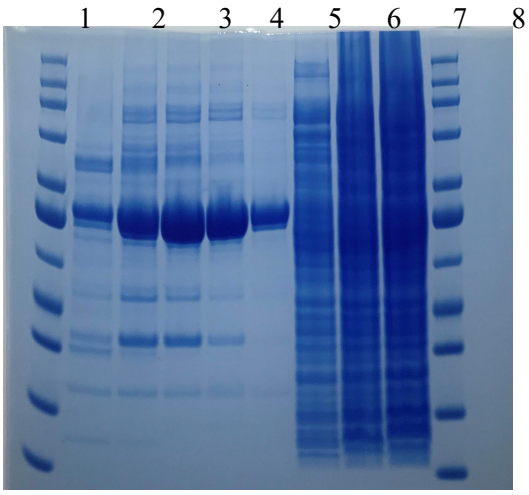

B

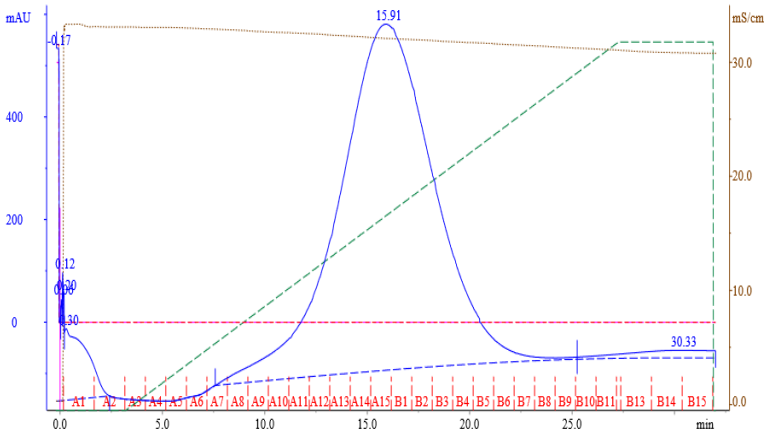

Figure A2 . Protein Purification of OleT$_{JE}$ from C41 (DE3).

A) SDS PAGE of the OleT$_{JE}$ purification. Wells 1-5 are OleT$_{JE}$ eluent, 6 is the Wash Fraction, 7 Flow Through and 8 Lysate.

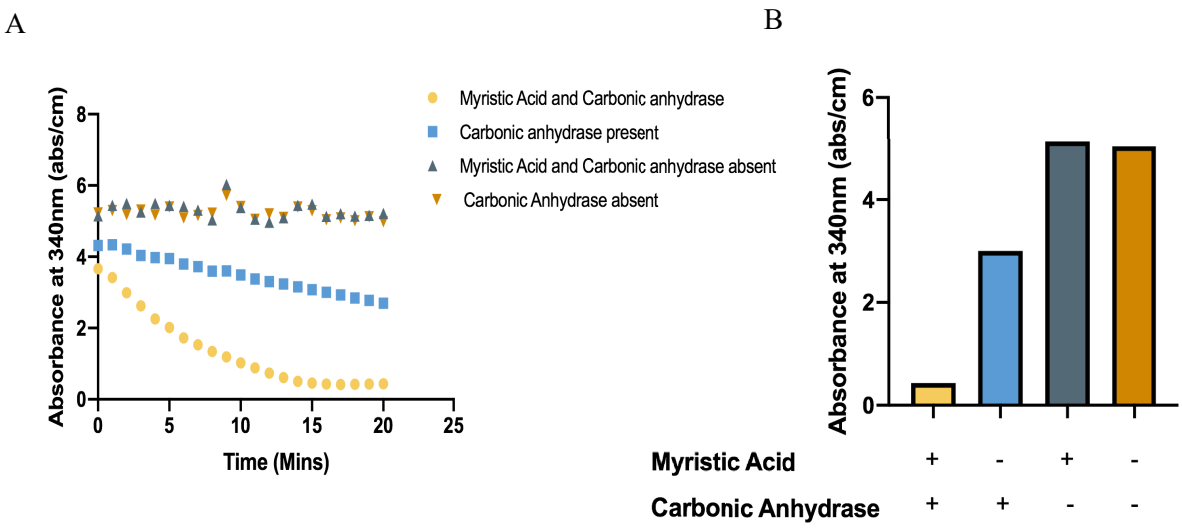

Figure A3. The PEPC-MDH Assay Screen with carbonic anhydrase.
A) Continuous curve of OleT assay in the presence or absence of carbonic anhydrase and myristic acid. B) End point of the same reaction as A, at 15mins.

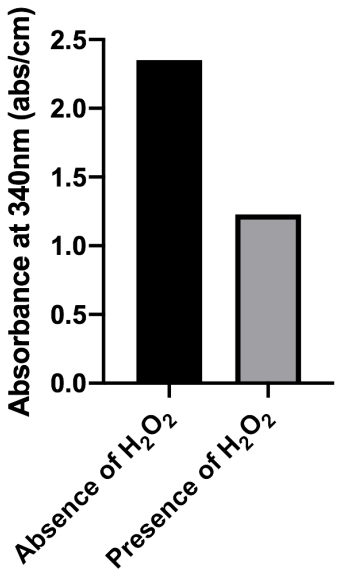

Figure A4. The $OleT_{JE}$ Assay in the presence and absence of H_2O_2

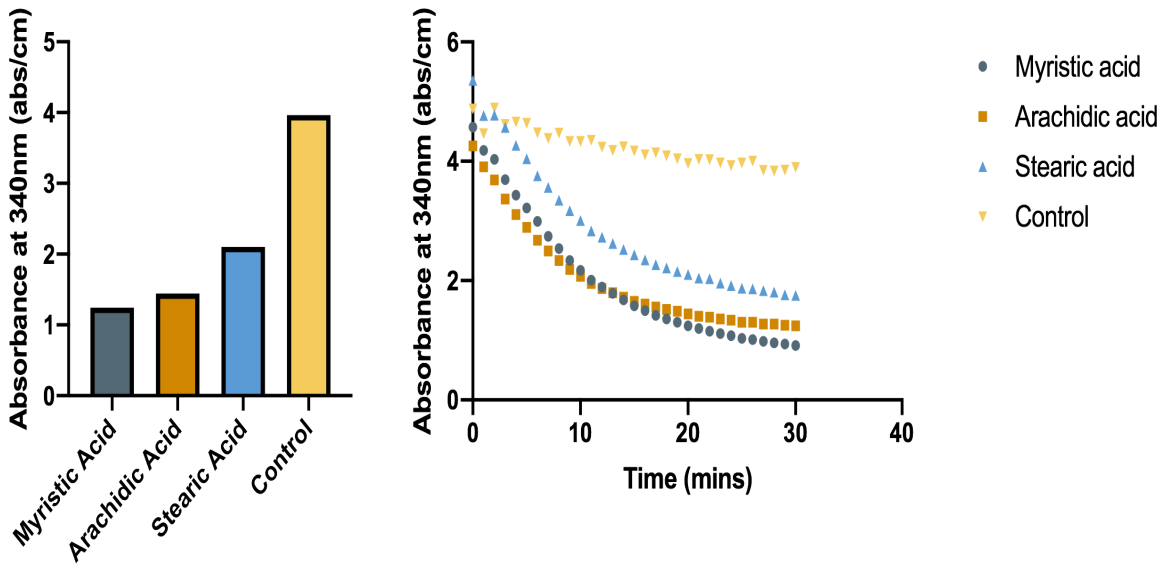

Figure A5. The OleT$_{JE}$ Assay with different substrates.
A) Endpoint of different substrates and control at 30mins B) Time-course of different substrates and a negative control

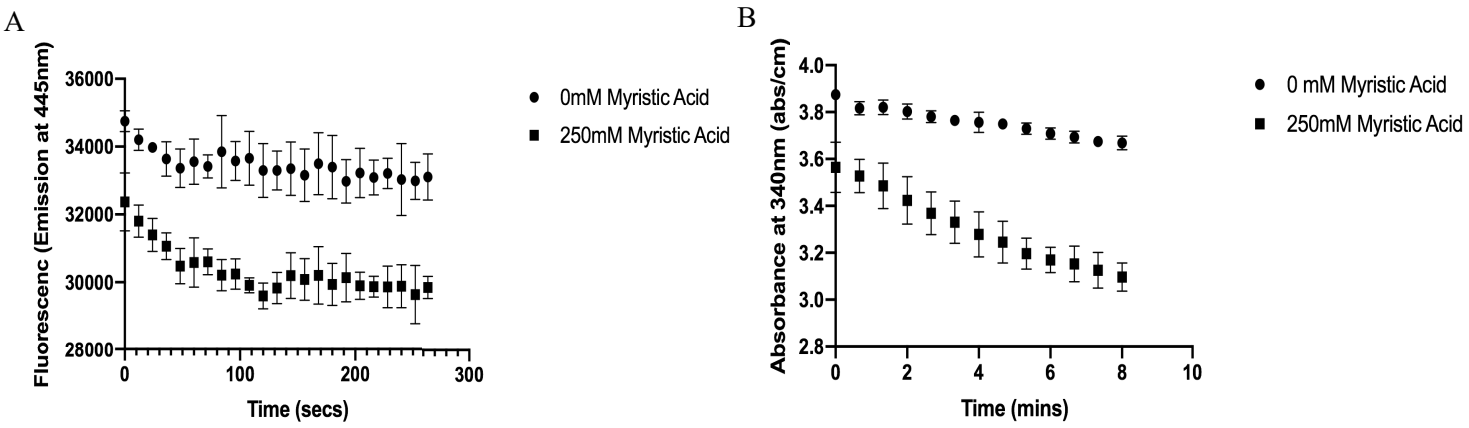

Figure A6. The detection of NADH oxidation using absorbance or fluorescence.
The OleT $_{JE}$ assay in duplicate with 250 μM of Myristic acid(substrate) measured through A) Fluorescence or B) Absorbance.

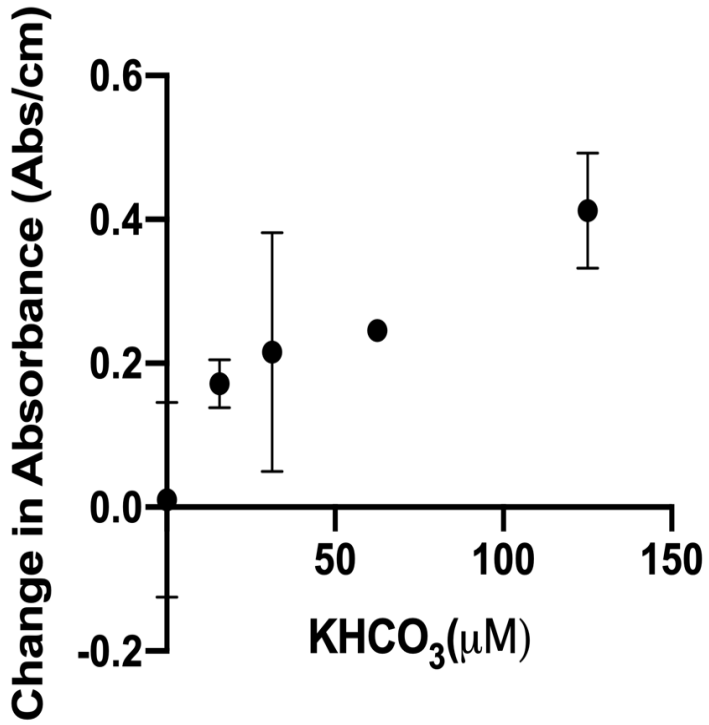

Figure A7. **The sensitivity of PEPC-MDH Assay.**
Preliminary experiments using 0.5mg/mL of PEPC and MDH (5x more than used), the noise previously observed in the assay has decreased. There is a steady upward trend as $KHCO_3$ is decreased (duplicates).

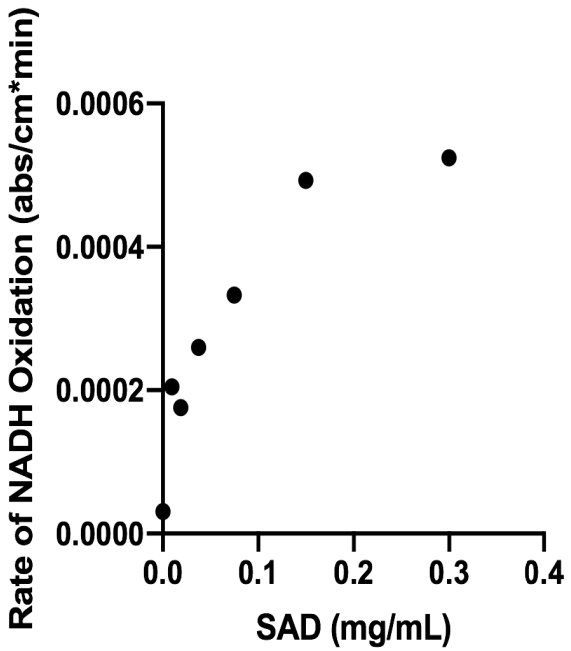

Figure A8. The effect of varying SAD concentration on the rate of NADH oxidation. The range where SAD is the limiting enzyme in the reaction can be detected in the linear region of the curve.

Appendix B: Common Media and Recipes

Table B1: Recipes of common media and buffers used in this thesis

Media and Buffers	Components	pH
LB	1% tryptone, 0.5% yeast extract, 0.5% sodium chloride	7
2YT	1.6% tryptone, 1% yeast extract, 0.5% sodium chloride	7
Lysis buffer	50mM sodium phosphate, 300mM sodium chloride, 10mM imidazone 10% glyrcerol	8
Wash buffer	50mM sodium phosphate, 300mM sodium chloride, 20mM imidazole, 10% glycerol	8
Elution Buffer	50mM sodium phosphate, 300mM sodium chloride, 250mM imidazome, 10% glycerol	8
Storage Buffer	100mM potassium phosphate, 750mM NaCl, 20% glycerol	8

References

Adkins, J., Pugh, S., McKenna, R., & Nielsen, D. R. (2012). Engineering microbial chemical factories to produce renewable "biomonomers." *Frontiers in Microbiology*, *3*(AUG), 1–12. https://doi.org/10.3389/fmicb.2012.00313

Agu, C. V., Lai, S. M., Ujor, V., Biswas, P. K., Jones, A., Gopalan, V., & Ezeji, T. C. (2018). Development of a high-throughput assay for rapid screening of butanologenic strains. *Scientific Reports*, *8*(1), 1–12. https://doi.org/10.1038/s41598-017-18074-7

Aharoni, A., Thieme, K., Chiu, C. P. C., Buchini, S., Lairson, L. L., Chen, H., … Withers, S. G. (2006). High-throughput screening methodology for the directed evolution of glycosyltransferases. *Nature Methods*, *3*(8), 609–614. https://doi.org/10.1038/nmeth899

Atsumi, S., Cann, A. F., Connor, M. R., Shen, C. R., Smith, K. M., Brynildsen, M. P., … Liao, J. C. (2008). Metabolic engineering of Escherichia coli for 1-butanol production. *Metabolic Engineering*, *10*(6), 305–311. https://doi.org/10.1016/j.ymben.2007.08.003

Atsumi, S., Hanai, T., & Liao, J. C. (2008). Non-fermentative pathways for synthesis of branched-chain higher alcohols as biofuels. *Nature*, *451*(7174), 86–89. https://doi.org/10.1038/nature06450

Axelsson, L., Franzén, M., Ostwald, M., Berndes, G., Lakshmi, G., & Ravindranath, N. H. (2012). Biotechnological advances in lactic acid production by lactic acid bacteria: lignocellulose as novel substrate. *Biofuels, Bioproducts and Biorefining*, *6*(3), 246–256. https://doi.org/10.1002/bbb

Barahona, E., Jiménez-Vicente, E., & Rubio, L. M. (2016). Hydrogen overproducing nitrogenases obtained by random mutagenesis and high-throughput screening. *Scientific Reports*, *6*(38291), 1–10. https://doi.org/10.1038/srep38291

Barker, H. A., & Taha, S. M. (1941). Clostridium kluyverii, an organism concerned in the formation of caproic acid from ethyl alcohol, (1), 347–363.

Barry, S. M., & Challis, G. L. (2012). *Tailoring Reactions Catalyzed by Heme-Dependent Enzymes : Spectroscopic Characterization of the L -Tryptophan-Nitrating Cytochrome P450 TxtE*. *Natural product biosynthesis by microorganisms and plants Part B* (1st ed., Vol. 516). Elsevier Inc. https://doi.org/10.1016/B978-0-12-394291-3.00001-0

Belcher, J., McLean, K. J., Matthews, S., Woodward, L. S., Fisher, K., Rigby, S. E. J., … Munro, A. W. (2014). Structure and biochemical properties of the alkene producing cytochrome p450 OleTJE (CYP152l1) from the jeotgalicoccus sp. 8456 bacterium. *Journal of Biological Chemistry*, *289*(10), 6535–6550. https://doi.org/10.1074/jbc.M113.527325

Betts, K. (2015). How Industrial Applications in Green Chemistry Are Changing Our World. *American Chemical Society*, 32. Retrieved from https://www.acs.org/content/dam/acsorg/membership/acs/benefits/extra-insights/green-chemistry-applications.pdf

Bogaert, I. N. A. Van, Groeneboer, S., Saerens, K., & Soetaert, W. (2011). The role of cytochrome P450 monooxygenases in microbial fatty acid metabolism, *278*, 206–221. https://doi.org/10.1111/j.1742-4658.2010.07949.x

Bojarra, S., Reichert, D., & Grote, M. (2018). Bio-based a , w -Functionalized Hydrocarbons from Multi- step Reaction Sequences with Bio- and Metallo-catalysts Based on the Fatty Acid Decarboxylase OleT JE, 1192–1201. https://doi.org/10.1002/cctc.201701804

Bridger, A., Biochemistry, D., Alberta, U., & Tg, C. (1980). The kinetic properties of phosphoenolpyruvate carboxykinase of Escherichia colil.

Bush, E., & Flato, G. (2019). *Canada's Changing Climate Report*.

Cheong, S., Clomburg, J. M., & Gonzalez, R. (2016). Energy-and carbon-efficient synthesis of functionalized small molecules in bacteria using non-decarboxylative Claisen condensation reactions. *Nature Biotechnology*, *34*(5), 556–561. https://doi.org/10.1038/nbt.3505

Church, G. M., Elowitz, M. B., Smolke, C. D., Voigt, C. A., & Weiss, R. (2014). Realizing the potential of synthetic biology. *Nature Reviews Molecular Cell Biology*, *15*(4), 289–294. https://doi.org/10.1038/nrm3767

Clean Fuel Steering Committee. (2019). Clean Fuels Investment in Canada, (November).

Dellomonaco, C., Clomburg, J. M., Miller, E. N., & Gonzalez, R. (2011). Engineered reversal of the β-oxidation cycle for the synthesis of fuels and chemicals. *Nature*, *476*(7360), 355–359. https://doi.org/10.1038/nature10333

Doppalapudi, S., Jain, A., Khan, W., & Domb, A. J. (2014). Biodegradable polymers-an overview. *Polymers for Advanced Technologies*, *25*(5), 427–435. https://doi.org/10.1002/pat.3305

Eriksson, E., & Welander, P. (1955). On a Mathematical Model of the Carbon Cycle in Nature. *Tellus*, *8*(2), 71. https://doi.org/10.1177/003754977803100208

Fang, B., Xu, H., Liu, Y., Qi, F., Zhang, W., Chen, H., … Li, S. (2017). Mutagenesis and redox partners analysis of the P450 fatty acid decarboxylase OleTJE. *Scientific Reports*, *7*(January), 44258. https://doi.org/10.1038/srep44258

Fernandes, J. C. B., Neto, G. D. O., Kubota, L. T., & Katekawa, E. (1998). Study of NADH Stability Using Ultraviolet ± Visible Spectrophotometric Analysis and Factorial Design, *55*, 50–55.

Fillet, S., & Adrio, J. L. (2016). Microbial production of fatty alcohols. *World Journal of Microbiology and Biotechnology*, *32*(9). https://doi.org/10.1007/s11274-016-2099-z

Ford, J. D. (2009). Vulnerability of Inuit food systems to food insecurity as a consequence of climate change: A case study from Igloolik, Nunavut. *Regional Environmental Change*, *9*(2), 83–100. https://doi.org/10.1007/s10113-008-0060-x

Gardner, T. S., Cantor, C. R., & Collins, J. J. (2000). Construction of a genetic toggle switch in Escherichia coli. *Letters to Nature*, *403*, 339–342.

Garrison, T. F., Murawski, A., & Quirino, R. L. (2016). Bio-based polymers with potential for biodegradability. *Polymers*, *8*(7), 1–22. https://doi.org/10.3390/polym8070262

Gautschi, E., Shrutkowski, A., Kronkaitis, A., Brown, M., Kabcenell, A., & Rajotte, D. (2006). Development of a High-Throughput Assay to Measure Histidine Decarboxylase Activity. *Society for Biomolecular Sciences*, 816–821. https://doi.org/10.1177/1087057106290803

Hajbabaei, M., Karavalakis, G., Miller, J. W., Villela, M., Xu, K. H., & Durbin, T. D. (2013). Impact of olefin content on criteria and toxic emissions from modern gasoline vehicles. *Fuel*, *107*, 671–679. https://doi.org/10.1016/j.fuel.2012.12.031

Hamad, K., Kaseem, M., Ayyoob, M., Joo, J., & Deri, F. (2018). Polylactic acid blends: The future of green, light and tough. *Progress in Polymer Science*, *85*, 83–127. https://doi.org/10.1016/j.progpolymsci.2018.07.001

Hammerer, L., Winkler, C. K., & Kroutil, W. (2018). Regioselective Biocatalytic Hydroxylation of Fatty Acids by Cytochrome P450s. *Catalysis Letters*, *148*(3), 787–812. https://doi.org/10.1007/s10562-017-2273-4

Hernández, N., Williams, R. C., & Cochran, E. W. (2014). The battle for the “green” polymer.

Different approaches for biopolymer synthesis: Bioadvantaged vs. bioreplacement. *Organic and Biomolecular Chemistry*, *12*(18), 2834–2849. https://doi.org/10.1039/c3ob42339e

Hu, Y., Zhu, Z., Nielsen, J., & Siewers, V. (2019). Engineering Saccharomyces cerevisiae cells for production of fatty acid-derived biofuels and chemicals. *Open Biology*, *9*(5). https://doi.org/10.1098/rsob.190049

Iwata, T. (2015). Biodegradable and bio-based polymers: Future prospects of eco-friendly plastics. *Angewandte Chemie - International Edition*, *54*(11), 3210–3215. https://doi.org/10.1002/anie.201410770

Jain, J. P., Sokolsky, M., Kumar, N., & Domb, A. J. (2008). Fatty acid based biodegradable polymer. *Polymer Reviews*, *48*(1), 156–191. https://doi.org/10.1080/15583720701834232

Jiang, W., Gu, P., & Zhang, F. (2018a). Steps towards ‘ drop-in ’ biofuels : focusing on metabolic pathways. *Current Opinion in Biotechnology*, *53*, 26–32. https://doi.org/10.1016/j.copbio.2017.10.010

Jiang, W., Gu, P., & Zhang, F. (2018b). Steps towards ‘drop-in’ biofuels: focusing on metabolic pathways. *Current Opinion in Biotechnology*, *53*, 26–32. https://doi.org/10.1016/j.copbio.2017.10.010

Kourist, R., Guterl, J. K., Miyamoto, K., & Sieber, V. (2014). Enzymatic decarboxylation-An emerging reaction for chemicals production from renewable resources. *ChemCatChem*, *6*(3), 689–701. https://doi.org/10.1002/cctc.201300881

Ladygina, N., Dedyukhina, E. G., & Vainshtein, M. B. (2006). A review on microbial synthesis of hydrocarbons. *Process Biochemistry*, *41*(5), 1001–1014. https://doi.org/10.1016/j.procbio.2005.12.007

Lakowicz, J. R., & Lakowicz, J. R. (1999). *Fluorescence Sensing*. *Principles of Fluorescence Spectroscopy*. https://doi.org/10.1007/978-1-4757-3061-6_19

Lamsen, E. N., & Atsumi, S. (2012). Recent progress in synthetic biology for microbial production of C3-C10 alcohols. *Frontiers in Microbiology*, *3*(JUN), 1–13. https://doi.org/10.3389/fmicb.2012.00196

Langer, R. (1990). New methods of drug delivery. *Science*, *249*(4976), 1527–1533. https://doi.org/10.1126/science.2218494

Lee, S. K., Chou, H., Ham, T. S., Lee, T. S., & Keasling, J. D. (2008). Metabolic engineering of

microorganisms for biofuels production: from bugs to synthetic biology to fuels. *Current Opinion in Biotechnology*, *19*(6), 556–563. https://doi.org/10.1016/j.copbio.2008.10.014

Li, F., Yang, K., Xu, Y., Qiao, Y., Yan, Y., & Yan, J. (2019). A genetically-encoded synthetic self-assembled multienzyme complex of lipase and P450 fatty acid decarboxylase for efficient bioproduction of fatty alkenes. *Bioresource Technology*, *272*(September 2018), 451–457. https://doi.org/10.1016/j.biortech.2018.10.067

Li, S., Cai, L., Wu, L., Zeng, G., Chen, J., Wu, Q., & Chen, G. Q. (2014). Microbial synthesis of functional homo-, random, and block polyhydroxyalkanoates by β-oxidation deleted Pseudomonas entomophila. *Biomacromolecules*, *15*(6), 2310–2319. https://doi.org/10.1021/bm500669s

Li, T., Huo, L., Pulley, C., & Liu, A. (2012). Decarboxylation mechanisms in biological system. *Bioorganic Chemistry*, *43*, 2–14. https://doi.org/10.1016/j.bioorg.2012.03.001

Liao, C., Wang, Y., Tan, X., Sun, L., & Liu, S. (2015). Discovery of novel inhibitors of human S-adenosylmethionine decarboxylase based on in silico high-throughput screening and a non-radioactive enzymatic assay. *Nature Publishing Group*, (June), 1–11. https://doi.org/10.1038/srep10754

Liao, J. C., Mi, L., Pontrelli, S., & Luo, S. (2016). Fuelling the future: Microbial engineering for the production of sustainable biofuels. *Nature Reviews Microbiology*, *14*(5), 288–304. https://doi.org/10.1038/nrmicro.2016.32

Liu, K., & Li, S. (2020). Biosynthesis of fatty acid-derived hydrocarbons: perspectives on enzymology and enzyme engineering. *Current Opinion in Biotechnology*, *62*, 7–14. https://doi.org/10.1016/j.copbio.2019.07.005

Liu, M., Sergienko, E. A., Guo, F., Wang, J., Tittmann, K., Hübner, G., … Jordan, F. (2001). Catalytic acid - Base groups in yeast pyruvate decarboxylase. 1. Site-directed mutagenesis and steady-state kinetic studies on the enzyme with the D28A, H114F, H115F, and E477Q substitutions. *Biochemistry*, *40*(25), 7355–7368. https://doi.org/10.1021/bi002855u

Liu, Yi, Wang, C., Yan, J., Zhang, W., Guan, W., Lu, X., & Li, S. (2014). Hydrogen peroxide-independent production of α-alkenes by OleTJE P450 fatty acid decarboxylase. *Biotechnology for Biofuels*, *7*(1), 28. https://doi.org/10.1186/1754-6834-7-28

Liu, Yilan, Chen, S., Chen, J., Zhou, J., Wang, Y., Yang, M., … Ma, Y. (2016). High production

of fatty alcohols in Escherichia coli with fatty acid starvation. *Microbial Cell Factories*, *15*(1), 1–10. https://doi.org/10.1186/s12934-016-0524-5

Markel, U., Lanvers, P., Sauer, D. F., Wittwer, M., Dhoke, G. V., Davari, M. D., … Schwaneberg, U. (2020). A photoclick-based high-throughput screening for the directed evolution of decarboxylase OleT. *Chemistry – A European Journal*. https://doi.org/10.1002/chem.202003637

Matte, A., & Grosse, S. (2010). Structural analysis of Bacillus pumilus phenolic acid decarboxylase , a lipocalin-fold enzyme, 1407–1414. https://doi.org/10.1107/S174430911003246X

Matthews, S., Belcher, J. D., Tee, K. L., Girvan, H. M., McLean, K. J., Rigby, S. E. J., … Munro, A. W. (2017). Catalytic determinants of alkene production by the cytochrome P450 peroxygenase OleTJE. *Journal of Biological Chemistry*, *292*(12), 5128–5143. https://doi.org/10.1074/jbc.M116.762336

McKenna, R., & Nielsen, D. R. (2011). Styrene biosynthesis from glucose by engineered E. coli. *Food, Pharmaceutical and Bioengineering Division - Core Programming Topic at the 2011 AIChE Annual Meeting*, *1*(5), 340–350. https://doi.org/10.1016/j.ymben.2011.06.005

Mendez-perez, D., Herman, N. A., & Pfleger, F. (2014). A desaturase gene involved in the formation of 1,14-nonadecadiene in Synechococcus sp. strain PCC 7002. *Applied and Environmental Microbiology*, *80*(19), 6073–6079. https://doi.org/10.1128/AEM.01615-14

Middleton, J., Cunsolo, A., Jones-Bitton, A., Shiwak, I., Wood, M., Pollock, N., … Harper, S. L. (2020). “We’re people of the snow:” Weather, climate change, and Inuit mental wellness. *Social Science and Medicine*, *262*(June), 113137. https://doi.org/10.1016/j.socscimed.2020.113137

Misra, A. K., & Verma, M. (2013). A mathematical model to study the dynamics of carbon dioxide gas in the atmosphere. *Applied Mathematics and Computation*, *219*(16), 8595–8609. https://doi.org/10.1016/j.amc.2013.02.058

Mitchell, M. J., Jensen, O. E., Cliffe, K. A., & Maroto-Valer, M. M. (2010). A model of carbon dioxide dissolution and mineral carbonation kinetics. *Proceedings of the Royal Society A: Mathematical, Physical and Engineering Sciences*, *466*(2117), 1265–1290. https://doi.org/10.1098/rspa.2009.0349

Mødici, R., María, D. De, Otten, L. G., & Straathof, A. J. J. (2011). A High-Throughput Screening Assay for Amino Acid Decarboxylase Activity. *Adv. Synth Catal*, *353*, 2369–2376. https://doi.org/10.1002/adsc.201100386

Morley, K. L., Grosse, S., Leisch, H., & Lau, P. C. K. (2013). Antioxidant canolol production from a renewable feedstock via an engineered decarboxylase. *Green Chemistry*, *15*(12), 3312–3317. https://doi.org/10.1039/c3gc40748a

Munro, A. W., McLean, K. J., Grant, J. L., & Makris, T. M. (2018). Structure and function of the cytochrome P450 peroxygenase enzymes. *Biochemical Society Transactions*, *46*(1), 183–196. https://doi.org/10.1042/BST20170218

Napper, A. D., & Sivendran, S. (2011). Miniaturized High-Throughput Fluorescent Assay for Conversion of NAD(P)H to NAD(P). *Current Protocols in Chemical Biology*, *3*(2), 81–97. https://doi.org/10.1002/9780470559277.ch100155

Nazrul Islam, S., & Winkel, J. (2018). Climate change and social inequality. *UN/DESA Working Papers*, (Report No. 152), 1–247. https://doi.org/10.4324/9781315103358

Nomura, C. T., & Taguchi, S. (2007). PHA synthase engineering toward superbiocatalysts for custom-made biopolymers, 969–979. https://doi.org/10.1007/s00253-006-0566-4

Power, I. M., Harrison, A. L., Dipple, G. M., & Southam, G. (2013). Carbon sequestration via carbonic anhydrase facilitated magnesium carbonate precipitation. *International Journal of Greenhouse Gas Control*, *16*, 145–155. https://doi.org/10.1016/j.ijggc.2013.03.011

Qiu, Y., Tittiger, C., Wicker-Thomas, C., Le Goff, G., Young, S., Wajnberg, E., … Feyereisen, R. (2012). An insect-specific P450 oxidative decarbonylase for cuticular hydrocarbon biosynthesis. *Proceedings of the National Academy of Sciences of the United States of America*, *109*(37), 14858–14863. https://doi.org/10.1073/pnas.1208650109

Rude, M. A., Baron, T. S., Brubaker, S., Alibhai, M., Del Cardayre, S. B., & Schirmer, A. (2011). Terminal olefin (1-alkene) biosynthesis by a novel P450 fatty acid decarboxylase from Jeotgalicoccus species. *Applied and Environmental Microbiology*, *77*(5), 1718–1727. https://doi.org/10.1128/AEM.02580-10

Rui, Z., Li, X., Zhu, X., Liu, J., Domigan, B., Barr, I., … Zhang, W. (2014). Microbial biosynthesis of medium-chain 1-alkenes by a nonheme iron oxidase. *Proceedings of the National Academy of Sciences of the United States of America*, *111*(51), 18237–18242.

https://doi.org/10.1073/pnas.1419701112

Savage, N. (2011). The ideal biofuel. *Nature*, *474*(7352), 9–11. https://doi.org/10.1038/474S09a

Sawyer, R. F. (1993). Trends in auto emissions and gasoline composition. *Environmental Health Perspectives*, *101*(SUPPL. 6), 5–12. https://doi.org/10.1289/ehp.93101s65

Schlegel, S., Genevaux, P., & de Gier, J. W. (2017). Isolating Escherichia coli strains for recombinant protein production. *Cellular and Molecular Life Sciences*, *74*(5), 891–908. https://doi.org/10.1007/s00018-016-2371-2

Schrimer, A., Rude, M., Li, X., Popova, E., & Del Cardayre, S. B. (2010). Microbial Biosynthesis of Alkanes. *Science*, *329*(July), 559–562.

Shen, C. R., & Liao, J. C. (2008). Metabolic engineering of Escherichia coli for 1-butanol and 1-propanol production via the keto-acid pathways. *Metabolic Engineering*, *10*(6), 312–320. https://doi.org/10.1016/j.ymben.2008.08.001

Shen, Claire R., Lan, E. I., Dekishima, Y., Baez, A., Cho, K. M., & Liao, J. C. (2011). Driving forces enable high-titer anaerobic 1-butanol synthesis in Escherichia coli. *Applied and Environmental Microbiology*, *77*(9), 2905–2915. https://doi.org/10.1128/AEM.03034-10

Shen, R., Cai, L. W., Meng, D. C., Wu, L. P., Guo, K., Dong, G. X., … Chen, G. Q. (2014). Benzene containing polyhydroxyalkanoates homo- and copolymers synthesized by genome edited Pseudomonas entomophila. *Science China Life Sciences*, *57*(1), 4–10. https://doi.org/10.1007/s11427-013-4596-8

Smithson, D. C., Shelat, A. A., Baldwin, J., Phillips, M. A., & Guy, R. K. (2010). Optimization of a non-radioactive high-throughput assay for decarboxylase enzymes. *Assay and Drug Development Technologies*, *8*(2), 175–185. https://doi.org/10.1089/adt.2009.0249

Sorigué, D., Légeret, B., Cuiné, S., Blangy, S., Moulin, S., Billon, E., … Beisson, F. (2017). An algal photoenzyme converts fatty acids to hydrocarbons. *Science (New York, N.Y.)*, *907*(September), 903–907.

Wang, J., Zhu, K., Ado, A. A. R., Ado, A. A. R., Ado, C. A. R., Ado, C. A. R., & Ado, D. O. X. (2018). Microbial production of alka (e) ne biofuels. *Current Opinion in Biotechnology*, *50*, 11–18.

Watts, N., Adger, W. N., Ayeb-Karlsson, S., Bai, Y., Byass, P., Campbell-Lendrum, D., … Costello, A. (2017). The Lancet Countdown: tracking progress on health and climate

change. *The Lancet*, *389*(10074), 1151–1164. https://doi.org/10.1016/S0140-6736(16)32124-9

Witkowski, A., Joshi, A. K., & Smith, S. (2002). Mechanism of the β-ketoacyl synthase reaction catalyzed by the animal fatty acid synthase. *Biochemistry*, *41*(35), 10877–10887. https://doi.org/10.1021/bi0259047

Wu, J., Zhang, X., Xia, X., & Dong, M. (2017). A systematic optimization of medium chain fatty acid biosynthesis via the reverse beta-oxidation cycle in Escherichia coli. *Metabolic Engineering*, *41*(February), 115–124. https://doi.org/10.1016/j.ymben.2017.03.012

Xia, Y., & Larock, R. C. (2010). Vegetable oil-based polymeric materials: Synthesis, properties, and applications. *Green Chemistry*, *12*(11), 1893–1909. https://doi.org/10.1039/c0gc00264j

Xiao, H., Bao, Z., & Zhao, H. (2015). High throughput screening and selection methods for directed enzyme evolution. *Industrial and Engineering Chemistry Research*, *54*(16), 4011–4020. https://doi.org/10.1021/ie503060a

Xu, H., Liang, W., Ning, L., Jiang, Y., Yang, W., Wang, C., … Li, S. (2020). Directed Evolution of P450 Fatty Acid Decarboxylases via High-Throughput Screening towards Improved Catalytic Activity. *ChemCatChem*, *12*(1), 80–84. https://doi.org/10.1002/cctc.201901347

Yan, J., Liu, Y., Wang, C., Han, B., & Li, S. (2015). Assembly of lipase and P450 fatty acid decarboxylase to constitute a novel biosynthetic pathway for production of 1-alkenes from renewable triacylglycerols and oils. *Biotechnology for Biofuels*, *8*, 34. https://doi.org/10.1186/s13068-015-0219-x

Yu, K., Hu, S., Huang, J., & Mei, L. (2011). Enzyme and Microbial Technology A high-throughput colorimetric assay to measure the activity of glutamate decarboxylase. *Enzyme and Microbial Technology*, *49*(3), 272–276. https://doi.org/10.1016/j.enzmictec.2011.06.007

Zhou, Y. J., Buijs, N. A., Zhu, Z., Gómez, D. O., Boonsombuti, A., Siewers, V., & Nielsen, J. (2016). Harnessing Yeast Peroxisomes for Biosynthesis of Fatty-Acid-Derived Biofuels and Chemicals with Relieved Side-Pathway Competition. *Journal of the American Chemical Society*, *138*(47), 15368–15377. https://doi.org/10.1021/jacs.6b07394